2016-05-06

Dynamic Analysis of a Light Wood-Framed Structure during Fire Conditions

Michael Figueroa
Worcester Polytechnic Institute

Dynamic Analysis of a Light Wood-Framed Structure during Fire Conditions

By
Michael Figueroa

A Thesis
Submitted to the Faculty
of the
WORCESTER POLYTECHNIC INSTITUTE
in partial fulfillment of the requirements for the
Degree of Master of Science
In
Civil Engineering
May 2016

APPROVED:

Professor Yeesock Kim, Major Advisor
Civil and Environmental Engineering

Professor Nicholas A. Dembsey, Co-Advisor
Fire Protection Engineering

Professor Leonard D. Albano, Co-Advisor
Civil and Environmental Engineering

Professor Tahar El-Korchi, Department Head
Civil and Environmental Engineering

Abstract

The purpose of this project is to create a theoretical dynamic analysis model to assess the dynamic response of light, wood-framed structures before and after fire conditions. This information is useful for predicting the damage to structural integrity due to a fire. The mass and stiffness matrices used for the dynamic model are derived from a standard residential building created for an existing project at WPI funded through the DHS/FEMA/USFA Assistance to Firefighters Grant program. The damping matrix is derived via the Rayleigh Damping Method using the mass and stiffness matrices obtained through SAP. Then, theoretical impact forces are applied to the developed dynamic model, and the acceleration response is estimated using Matlab. Both acceleration time history and frequency responses are used as the evaluation method. Finally, the dynamic model is integrated with a fire simulation model to investigate the impact of fire conditions on dynamic responses of residential buildings. The results show that frequencies can shift due to the structural degradation due to fire.

Table of Contents

Table of Figures

List of Tables

1. Introduction

1.1. Objective

The purpose of this research is to create a theoretical dynamic model to analyze a light, wood-framed structure before and after a fire. The structure was designed for an existing project at WPI funded through the DHS/FEMA/USFA Assistance to Firefighters Grant program **[1]**. This project focuses on typical two-story residential structures made of conventional, light, wood-framed construction. The primary goal is to create a theoretical model to predict the shift in dynamic response of a light, wood-framed structure before and after a fire. Acceleration and frequency response was the primary focus of this project. This information relates to failure prediction within wood structures during fire conditions.

1.2. Project Scope

The following list details the full scope of this research:

- Design a test specimen to represent typical, light, wood-framed, residential structures in the USA.
- Design a test rig to house the test specimen to be used for future experiments.
- Analyze possible vent configurations of the test compartment using FDS.
- Analyze thermal results, including temperature and heat flux, of the chosen compartment configuration using FDS.
- Create a structural, finite element model to obtain the mass, stiffness, and damping matrices needed for dynamic analysis.
- Create a structural dynamic model of the test specimen using Matlab.
- Apply thermal reduction theory to allow Matlab to perform structural dynamic analysis during fire conditions.
- Compare the theoretical dynamic response before and after a fire.

Following these steps, a dynamic model is created to predict the theoretical dynamic response of a light, wood-framed structure. Future testing is required to validate the dynamic model before and after a fire, which may be carried out by the DHS Green Building Project team at WPI. This project sets up the theoretical framework for future testing in structural dynamic testing of light, wood-framed structures.

1. Background

This project was a contribution to an existing project within the WPI Fire Protection Engineering Department which focuses on the *Quantification of Green Building Features on Firefighters*, which will be referred to throughout this report as the DHS Green Building Project. Funding for the original project came from the Department of Homeland Security (DHS). Their project was focused on creating a static, structural failure model for various green building methods of light, wood-framed residential structures. This project was able to collaborate with the DHS Green Building Project to investigate the dynamic, structural analysis response of their light, wood-framed test structure.

1.1. Historic Fire Data

Fires are major concerns for both human life and structural health. Based on a NFPA report on firefighter fatalities **[2]**, over half of the firefighter deaths (71 deaths in 2000 through 2009) occurred in one- and two- family dwellings, and as a result this type of residential building will be the focus of this study. The most prevalent cause of firefighter fatalities in structural fires is asphyxiation (57% of the total fatalities), and the major reasons which lead to these fatalities are: structural collapse (35%); the progress of fire, backdraft or flashover (31%); becoming lost inside the structure (23%) and other reasons. These statistics state the need for research to reduce the probability of structural failure and increase the use of structural health monitoring methods to predict structural damage during fires.

To understand a fire scenario, the fire must first be defined based on the characteristics of the specific fire. One such characteristic is known as flashover, which is defined as the point in time

in which all of the combustible materials within an area reach their ignition temperatures. An article in the *Fire Safety Journal* called “Defining Flashover for Fire Hazard Calculations” **[3]** defines approximate temperature of flashover as 600°C. Additionally, post-flashover fires have been an area of investigation in the fire protection field that are representative of large residential fires. The exact temperatures for post-flashover fires are still in debate, but studies have shown that it is generally close to 1000°C **[4]**. The DHS Green Building Project team chose to base their research on typical residential buildings during post-flashover conditions. The vent configurations chosen for both the DHS Green Building project and this research were designed to simulate post-flashover temperatures.

1.2. Construction Methods

In the U.S, most one- and two- family residential houses have been built using light, wood-framed construction techniques. Compared to conventional framing, advanced framing used in green building construction requires fewer studs and provides more space for insulation. The DHS Green Building Project investigated the differences between conventional framing, advanced framing, and structural insulated panels. This project limited the scope of construction methods to the traditional framing method for the dynamic analysis.

This project focuses on conventional wood frame construction, which consists of plywood attached to wood floor joists and 2” x 4” wood studs placed 16” on center. The spacing of the members creates structural redundancy that contributes to the overall strength and stiffness of the structures. Modern light, wood-framed houses are usually built using platform framing, in which floors would be built directly on top of the stud walls of the floors below. This replaced the

antiquated balloon framing that used studs that spanned from the ground all the way to the roof. This was an inefficient construction method due to the fact that it would allow fire to quickly spread between floors **[5].**

1.3. Material Properties

Wood is a natural material of anisotropic and cellular behavior. Its strength capacity varies significantly depending on the particular axis. Qualities that affect the yield strength and elastic modulus include the density, moisture content, temperature, and defects of the wood **[6].** Southern pine is one of the most common types of wood used for one-story and two-story residential structures in the USA, so it was used as the building material for this project. The table below shows the range of structural capacities for various grades of Southern Pine **[6]**.

Species and commercial grade	Size classification	Design values in pounds per square inch (psi)							Grading Rules Agency
		Bending F_b	Tension parallel to grain F_t	Shear parallel to grain F_v	Compression perpendicular to grain $F_{c\perp}$	Compression parallel to grain F_c	Modulus of Elasticity E	Modulus of Elasticity E_{min}	
SOUTHERN PINE									
Dense Select Structural		3,050	1,650	175	660	2,250	1,900,000	690,000	
Select Structural		2,850	1,600	175	565	2,100	1,800,000	660,000	
Non-Dense Select Structural		2,650	1,350	175	480	1,950	1,700,000	620,000	
No.1 Dense		2,000	1,100	175	660	2,000	1,800,000	660,000	
No.1	2" - 4" wide	1,850	1,050	175	565	1,850	1,700,000	620,000	
No.1 Non-Dense		1,700	900	175	480	1,700	1,600,000	580,000	
No.2 Dense		1,700	875	175	660	1,850	1,700,000	620,000	
No.2		1,500	825	175	565	1,650	1,600,000	580,000	
No.2 Non-Dense		1,350	775	175	480	1,600	1,400,000	510,000	
No.3 and Stud		850	475	175	565	975	1,400,000	510,000	

Figure 1 - Southern Pine Design Values

Every type of material has a unique response to fire. Wood is shown to degrade with respect to yield strength and elastic modulus during elevated temperatures. Trends in structural capacity degradation are shown in the graphs below **[7]**. It should be noted that the data in the graphs

below only apply to low temperatures and not the temperatures experienced during fires. The moisture content quickly evaporates during fire conditions, which significantly lowers the yield strength of the wood. Additionally, the cross-sectional area of the wood members is lost due to charring. Although the loss in cross-sectional area lowers the stiffness of the structure, the char layer actually acts as a natural insulator for the core of the affected members, thereby lowering the rate of charring over time **[8]**.

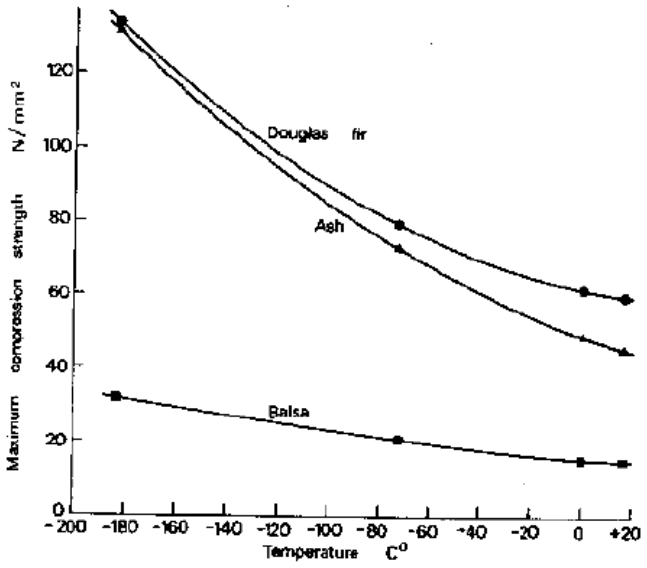

Figure 2 - Compressive Strength of Wood vs. Temperature

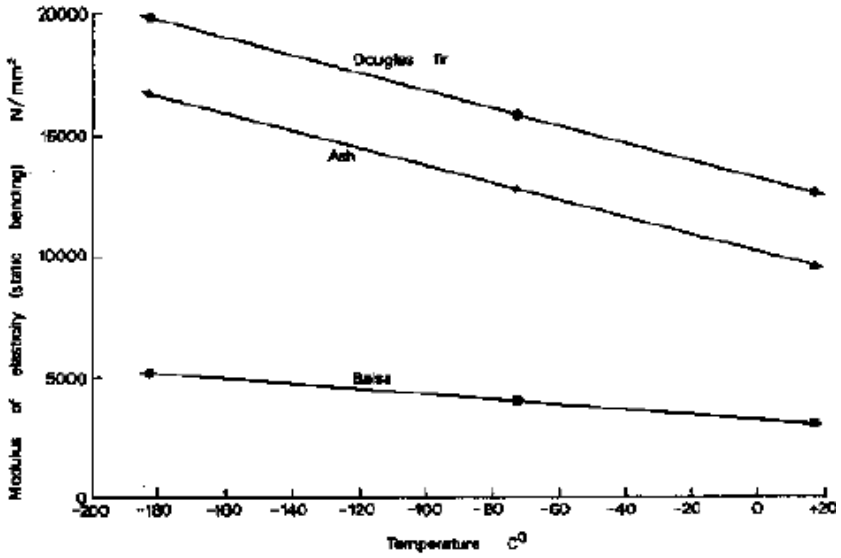

Figure 11.12 Effect of temperature on the modulus of elasticity of three species of timber. (From the Princes Risborough Laboratory, Building Research Establishment. © Crown copyright.)

Figure 3 - Elastic Modulus of Wood vs. Temperature

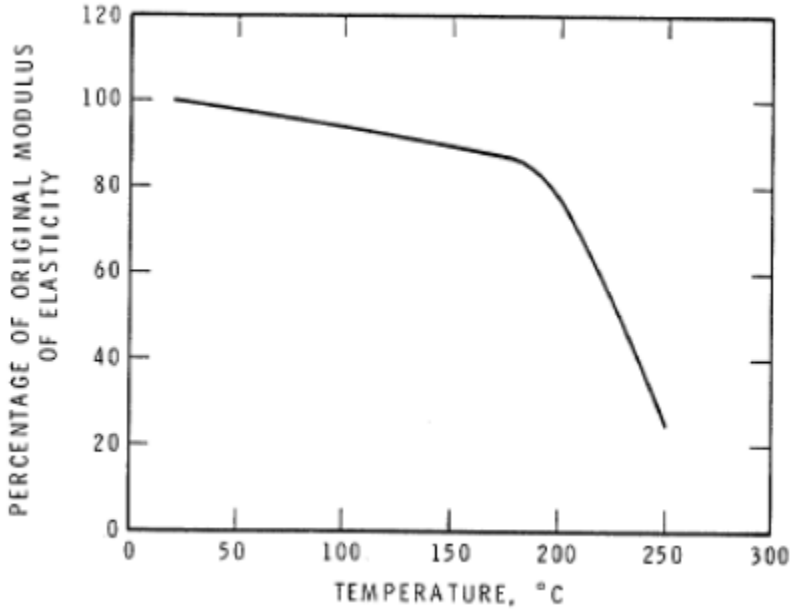

Figure 4 - Wood Elastic Modulus Ratio

The graph above shows the ratio of elastic modulus for wood as a function of temperature **[9]**. The elastic modulus affects the structural stiffness of members, so this information is useful for calculating temperature dependent stiffness. However, the study investigated material properties up to 250°C. Temperatures above this range causes wood to char, which significantly lowers the elastic modulus. Wood structural members can be assumed to have an inner core that is unaffected by fire for simplification of design. The charring effect essentially removes part of the cross-sectional area from the load carrying element. For that reason, the effect of degrading elastic modulus was excluded from the scope of investigation for this project.

Traditionally, post-flashover fires have been tested using ASTM E 119 **[11]** or ISO 834 **[12]** to establish the fire resistance rating of assemblies such as the compartment used for this project. The American Wood Council has published a document called *TR10 – Calculating the Fire Resistance Rating of Exposed Wood Members* **[13]**, which has simplified modern research in structural fire engineering into equations that can be used to calculate the structural capacity of wood members during fire conditions. Their method involves calculating the char rate based on exposure time in an E 119 fire and using that rate to calculate the new, reduced cross-sectional area of the members. The following equation is presented in that report.

$$\beta_{eff} = \frac{1.2\,\beta_n}{t^{0.187}}$$

Equation 1

Where: β_{eff} = effective char rate (in/hr) adjusted for exposure time, β_n = nominal char rate (in/hr), t = exposure time (hr)

A nominal char rate of 1.5 in/hr is often used as an accepted value for most wood material types. The methods presented in TR 10 present an effective, easy way to calculate the adjusted structural capacity of wood members based on degradation of geometry. That same method is adopted for this project, in which a char rate is calculated based on a given scenario and used to calculate new geometry. However, the methods presented in TR 10 assume a direct fire exposure in a standard E 119 fire, which is not typical of all residential fires. Instead, this project will use a new equation for char rate in conjunction with thermal data calculated using FDS.

Additionally, a report in the *Fire Safety Journal* by Babrauskas **[14]** details the advances in char rate research. Babrauskas suggests multiple new equations to calculate the char rate of wood members based on more specific details of a given scenario. The article mentioned that recent testing using cone calorimeters have yielded more detailed correlations between heat flux, exposure time, and char rate. The following equation was presented to yield a more accurate portrayal of char rate.

$$\beta = 0.23(\dot{q}''_{tot})^{0.5} t^{-0.3} \qquad \textbf{Equation 2}$$

Where: β = char rate, $\dot{q}''_{tot}$ = total external heat flux, t = exposure time

This equation allows char rate to be calculated for more specific fire scenarios, such as the fire used in this project. This equation was used with the heat flux data calculated in FDS to derive specific values of char rate at various time intervals in a simulated fire, which is detailed later in this report. Comparable values for char rate of floor panels can be found in Appendix C – Char Rates.

1.4. Structural Dynamics

The field of structural engineering has evolved substantially in terms of structural dynamics. The demand to design buildings to withstand dynamic forces such as wind and earthquakes has created research opportunities to better understand structural behavior when buildings are in motion. Historically, there have been many catastrophic events in which wind caused bridges to fail when the wind reached the same natural frequency as the bridge. Similarly, buildings have been critically damaged or have completely collapsed during major earthquakes. This devastating behavior has created the need for the field of structural health monitoring, in which advanced structural analysis is employed to assess the integrity of a structure before, during, and after a dynamic event. The methods used for this project investigate the dynamic response of the light, wood-framed structure before and after a fire.

One important variable to consider in dynamic analysis is acceleration data, which can be collected using accelerometers that are attached to a building. When the acceleration data is collected, it can be analyzed to derive the frequency of the response. The methods used in this project employ the state-space equations to calculate the acceleration response and the fast Fourier transform to derive the frequency. The matrices that are needed for the dynamic analysis are extracted from a structural analysis. The drawback is that the system and the results completely depend on the assumptions made when creating the analytical model. If there is not enough information about the structure readily available, then it is not possible to produce an accurate dynamic analysis model.

However, an article in the *Sound and Vibration Journal* suggested a new method of modal testing that does not require input parameters to perform structural dynamic analysis **[15]**. It tested a plate structure with well-defined modes, resonance frequencies, and damping values. These values were then estimated using only the measured response of the structure without artificial excitation. This method was successfully used for the measurement of dynamic response due to wind, but it could also be applied to scenarios in which the input force is not known. Although this method was not used for this project, it would be an excellent way to make a dynamic failure model following this research in the future. This project was also limited by the assumptions made in the creation of the structural analysis model, so a method such as this would allow a more accurate analysis to be developed.

2. Methodology

This section details the methodology that was used to create the dynamic model for this project. This includes the specimen design, the test rig design, the fire modeling analysis, and the reduction theory. The specimen was chosen to represent typical light, wood-framed construction in the USA, the test rig was designed to house the specimen for future testing, the fire model was needed to design the vents for future testing, and the reduction theory was developed in integrate the degradation effects of fire into the dynamic model.

2.1. Specimen Design

Before this project began, the DHS Green Building Project performed a yearlong investigation of green building techniques used in the United States. After the investigation, their team developed a model using Revit to represent typical light, wood-framed construction in the USA. The representative model that was created for their project is shown below.

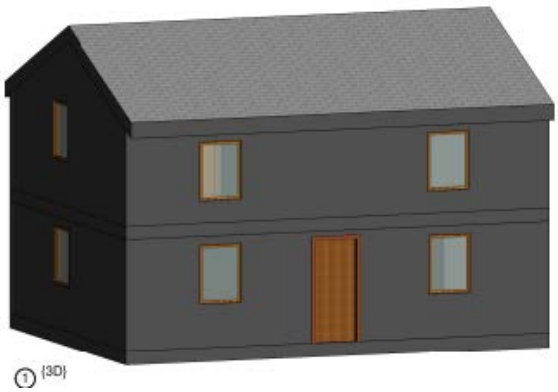

Figure 5 - Revit Model of Typical Residence

This structure is comprised of light frame, platform construction with 2” x 4” Southern Pine studs placed 16” on center. As a residential occupancy, ASCE 7-10 recommends a dead load of 20 psf and a live load of 40 psf **[18]**. These loads were used in conjunction with the *National Design Specification for Wood Construction* (NDS) to design the studs and joists within the structure **[6]**.

The intent of the DHS Green Building Project was to perform a full-scale structural fire test within the Gateway fire lab at WPI. Even with the size of the lab, it was not practical to test a full sized, two-story residential building for the sake of efficiency and safety. A study was performed to see if a condensed model could still represent the static structural response of the full two-story structure. Their team wanted to investigate whether the full structure would exhibit a planar structural response that could be replicated with the planar model. Planar structural response refers to stress distributions being relatively uniform between the spans of the studs and joists. A planar model would essentially be a planar slice of a full structure that would still exhibit similar stress results. This would allow a much smaller test specimen to be used in the lab that would still be representative of the full scale structure. The model below represents the condensed structure that was used to represent the full structure.

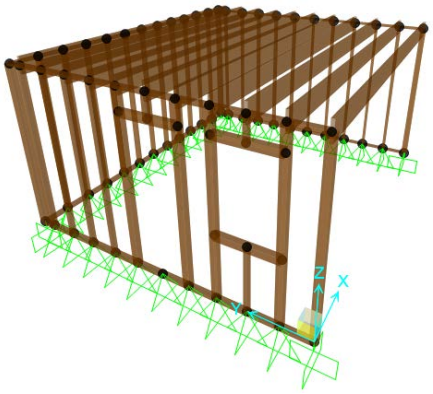

Figure 6 - SAP Model of Condensed Structure

The study performed for the DHS Green Building Project showed that the condensed structure accurately represented the static structural response of the full structure. The test structure acts as a single room of a full structure, and the same stress distributions could be seen if full scale loads were applied. The third wall was built to provide additional structural stability, which affects the vent configuration. Details regarding the vent analysis can be found later in this report. The following sections detail the ambient analysis that was used to compare the condensed and full structures. It was carried out for the DHS Green Building Project, and it allowed for a structural model to be created for use in the dynamic model used in this research. The following section summarizes the study that was previously performed for the DHS Green Building Project **[16]**.

It should be noted that the intent of this project was to collaborate with the DHS Green Building project to also use their test structure. Details of the differences in usage of the structure for static and dynamic load conditions can be found in subsequent sections of this report.

2.1.1. Ambient Analysis

The first step in determining proper research methods was to perform an ambient analysis of an example residence structure, which refers to a structural analysis using standard residential loads without a fire. The layout of the test home was originally chosen based on the investigation performed by Drew Martin and Young Geun You of the DHS Green Building Project team **[17]**. Based on their findings, the layout for the residence structure is a basic floor plan with two stories as shown below.

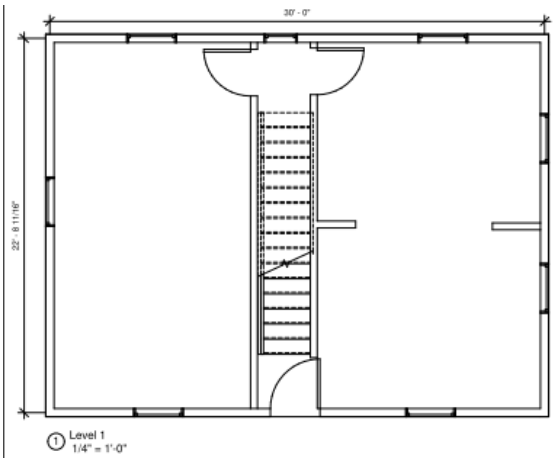

Figure 7 - First floor of residence structure

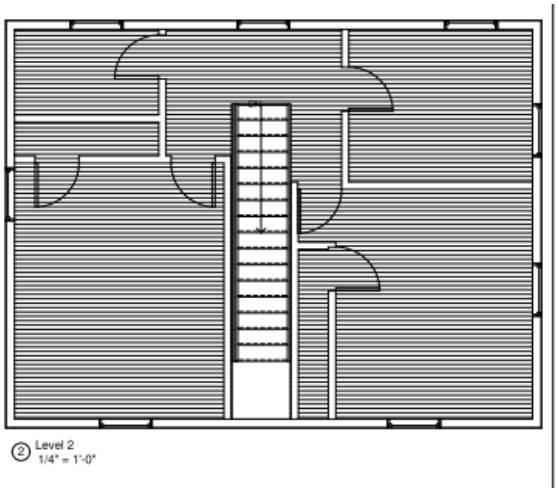

Figure 8 - Second floor of residence structure

The dimensions of this example residence structure are 30 feet by 22 feet with an 8-foot floor-to-ceiling height. The first floor is broken up into a living room, dining room, and kitchen. The second floor is divided into multiple bedrooms, and the two floors are connected by a staircase in the center of the building. The roof is a standard gable truss for simplicity of analysis purposes. The advanced light, wood-framed configuration (2” x 6” studs spaced 16” on center) was chosen as the baseline for the ambient analysis. It should be noted that the conventional light, wood-framed configuration was used for this project as it represents the structure that was initially built in the Gateway Fire Lab at WPI.

The goal of the ambient analysis was to verify that the overall residence structure could be modeled as a planar section. The model of the overall structure was simplified to be used with structural analysis software and hand calculations. Assumptions include simplified connections, consistent material properties, and static loads. The connections were chosen to be all pins, meaning that the rotational stiffness at each joint is essentially zero. This configuration was compared to a model with fully fixed connections. In reality, connections are considered to be somewhere between these two extremes, with a stiffness value that corresponds to the specific connection type. The connections used for this project were modeled as either pure pinned or pure fixed connections.

2.1.2. Design Loads

Based on the *Residential Structural Design Guide* **[19]**, the following loads were calculated for our particular scenario. This guide lists typical loads for various assemblies, including walls, floors, ceilings, sheathing, and insulation. Figure 9 represents the loads calculated for the entire area of each floor.

Floor 1		
D	20	psf
L	40	psf
Floor 2		
D	20	psf
L	30	psf
Attic		
D	15	psf
L	30	psf
Roof		
D	10	psf
S	55	psf
Wind		
1s	13.1	psf
2s	14.6	psf

Combinations	(psf)	**Floor 1**	**Floor 2**	**Attic**	**Roof**
1.4D		28	28	21	14
1.2D + 1.6L +0.5(Lr,S,R)		88	72	66	39.5
1.2D + 1.6(Lr,S,R) + (0.5L,0.8W)		44	39	33	111.68
1.2D + 1.6W + 0.5L + 0.5(Lr,S,R)		67.36	62.36	56.36	62.86
1.2D +- 1.0E + 0.5L + 0.2S		44	39	33	23
0.9D +- (1.6W,1.0E)		41.36	41.36	36.86	32.36
	Max	**88**	**72**	**66**	**111.68**

Figure 9 - LRFD Load Combinations

The figure above shows the applied design loads. These are typical design loads for a two-story residential structure. The loads were then factored based on the load combinations used in the Load and Resistance Factor Design (LRFD). This method of design compares required strength to actual strength with individual load factors for each load type such as dead, live, snow, and rain. In contrast, the factor of safety is normally associated with Allowable Stress Design (ASD).

For this research, gravity loads were the primary concern for investigation. Comparatively, the gravity loads had a much more significant effect on the structure than lateral loads. With common practice in LRFD, the load combination of greatest magnitude is chosen to design components of the structure. In this case, each individual floor was a component to be designed separately using the respective loads for that floor. The second load combination (1.2D + 1.6L) is the greatest magnitude for the 1st floor, 2nd floor, and attic. The third load combination (1.2D + 1.6S + 0.5L) is the greatest magnitude for the roof. The second load combination for LRFD (1.2D + 1.6L) was used to design the column studs to support the full load of the floors above. In this logic, the gravity loads have the greatest effect on the structural analysis.

Gravity loads were used to verify the condensation of the full structure by modeling the planar structural response. The addition of lateral loads was initially considered, but gravity loads were ultimately chosen to simplify the study. As is the case for structural design, the typical scenario is chosen as the baseline while neglecting the absolute worst case scenarios. For typical residential structures, designers look for the load combinations that are most common and relevant for a particular location. Gravity loads induced by snow normally have the greatest effect on structural performance. The DHS Green Building Project team chose to base the design location in New England and use the gravity loads that are most common in that region. Lateral loads were excluded from the scope of the project, but are a good topic for future research in structural analysis during fire conditions.

The scale of this research allows for the use of full-scale residential loads to test structural performance during a fire. The design loads are derived using the Load and Resistance Factor

Design (LRFD), which uses different factors for each load case to create design scenarios for proportioning the elements of a building. These factored loads define the limiting load conditions at failure, while unfactored loads represent service conditions. For this reason, unfactored loads are used to design a structure to its deflection limits, or level of serviceability comfort. For this research, the unfactored loads will be used to represent the service load conditions of the structure. The factored loads were not used as the DHS Green Building Project wanted to use smaller loads to test to a point just before failure.

Table 1 - Test Loads

Level	**Test Load (psf)**
Floor 1	60
Floor 2	50
Attic	45
Roof	65

2.1.3. Structural Model

A structural model was made for design and analysis purposes using SAP2000. This represents the structure consisting of the steel test rig and the wood specimens. For this report, a conventional light, wood-framed configuration (2” x 4” studs) was used to test the dynamic model. This software allowed the extraction of the mass and stiffness matrices in text format, which were later converted to cell format using Matlab. SAP2000 uses a lumped node mass method, which creates points of mass at each of the joints within the model.

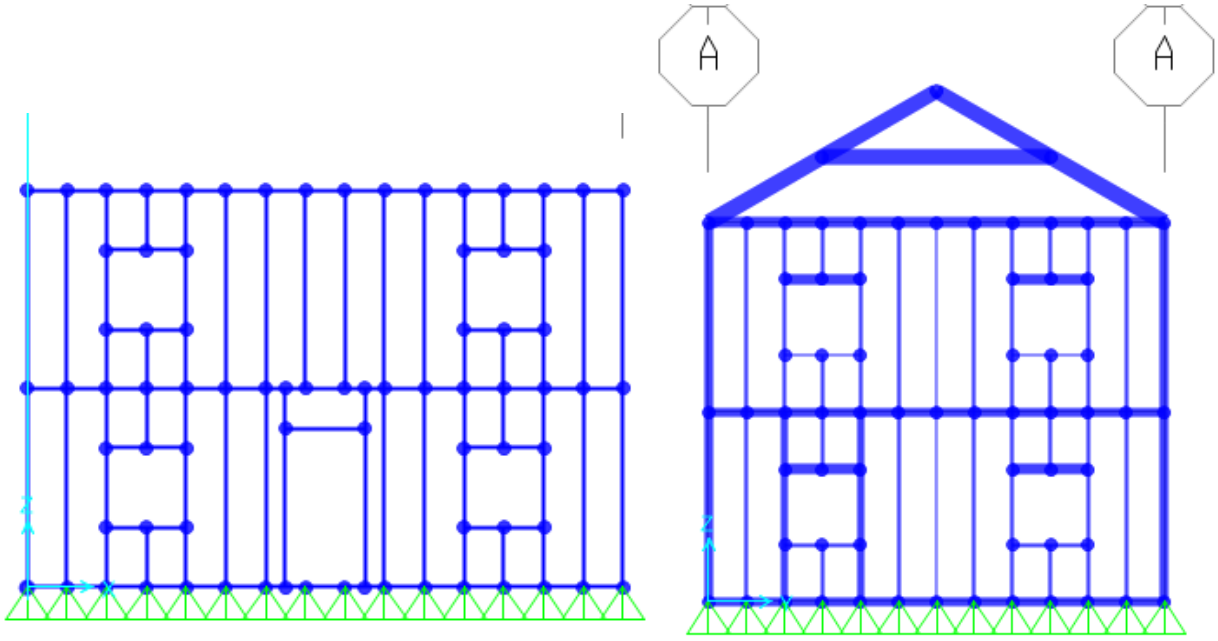

Figure 10 - Views of Full Structural Model

These figures show the model that was used in the structural analysis software SAP2000 **[20]**. The lines represent the members, and the external nodes represent the connections. Each construction configuration was used to test the planar feasibility of the structure. If the structural

performance of the overall residence structure matches the structural performance of the planar section, then the use of a planar section is feasible for testing purposes.

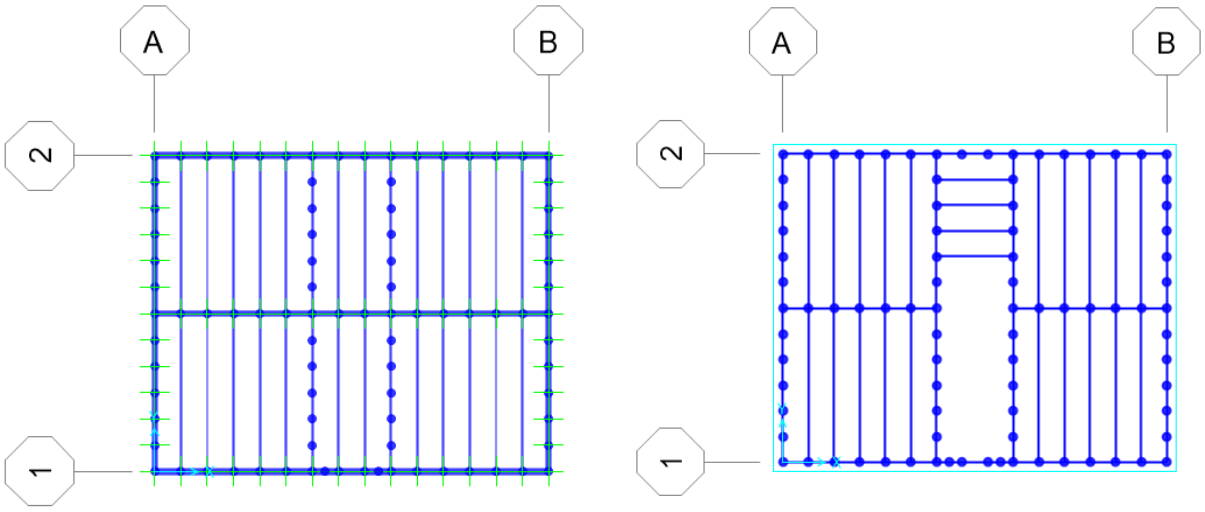

Figure 11 - Plan Views of Full Structural Model

2.1.4. Condensed Analysis

The DHS Green Building project required a test specimen that was smaller than a full-sized building in order to test in the WPI Gateway Fire Lab. A study was carried out to see if a condensed version of the building could still represent the behavior of the full-sized building for static, gravity loads in terms of moment and stress. Ultimately, it was shown that the condensed model represented the full-sized building for a static loading scenario. However, the condensed structure is not representative of the dynamic response of the full-sized building as the mass and stiffness were reduced due to the smaller size of the condensed structure. Although the condensed structure does not represent the magnitude of the structural dynamic response, it was chosen as the test structure for this thesis to have a theoretical structure to test the dynamic model. The condensed structure from the DHS Green Building Project was chosen for this project anticipating potential validation testing of dynamic response during fires in the future.

To investigate whether a smaller test structure could be used, a condensed model of the full structure was analyzed in SAP2000 using the chosen design loads and compared against the full structure. For design purposes, the factored loads were used to determine whether the selected members had the proper load bearing capacity. The stress profiles were compared between the full structure and the planar structure to see how they correlated. In the results view of SAP2000, the red represents the maximum stress induced by compression, and the blue represents the maximum stress induced by tension. The software scales the visible range of the stress to show the different magnitudes of stress; however, detailed results of the analysis can be found in the results table. The visual results of the structural analysis are shown below.

Full Residence Structure

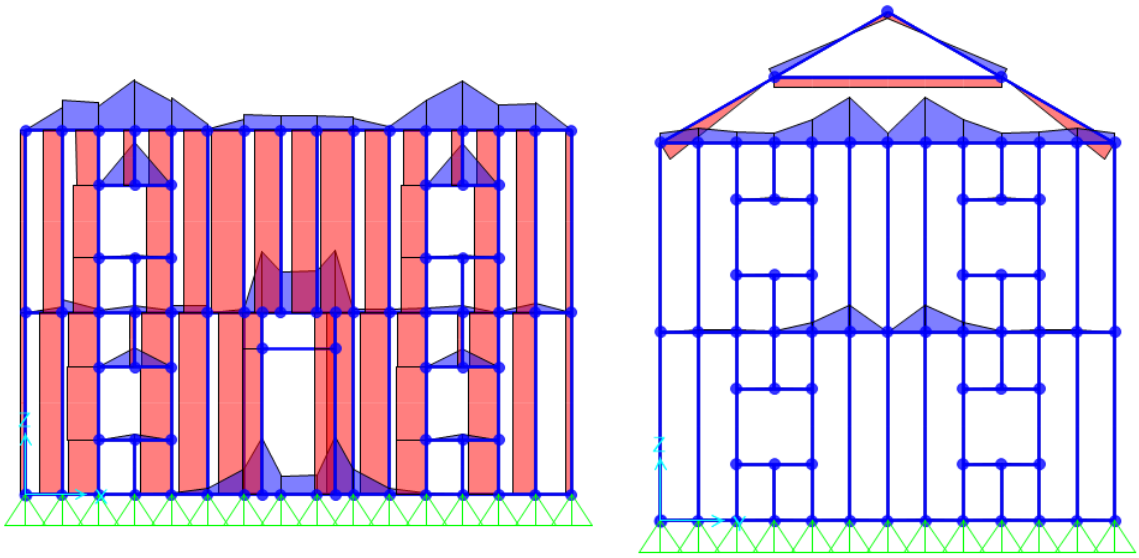

Figure 12 - Exterior Stress Results (Full Model)

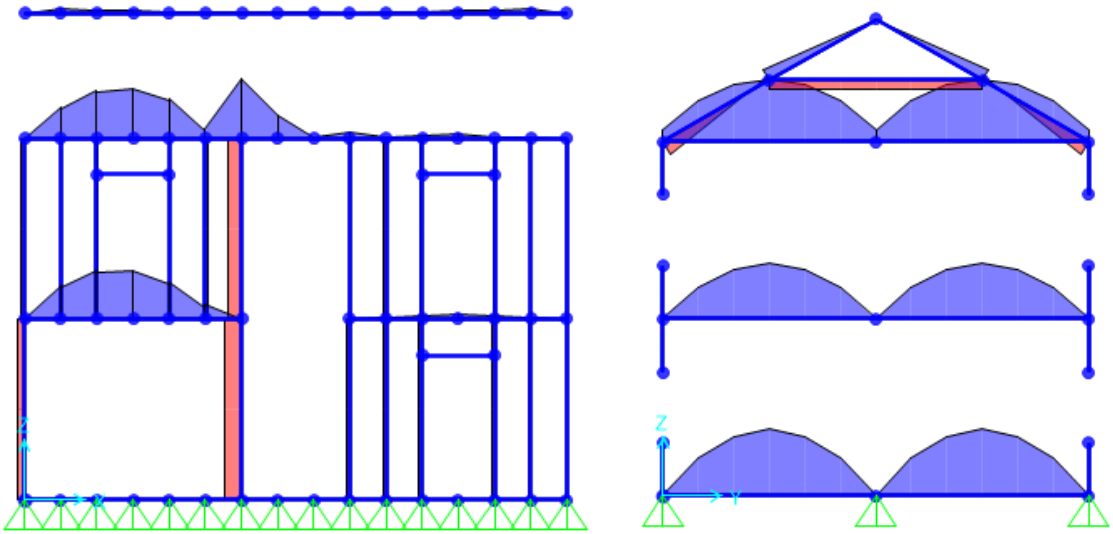

Figure 13 - Interior Stress Results (Full Model)

Planar Section

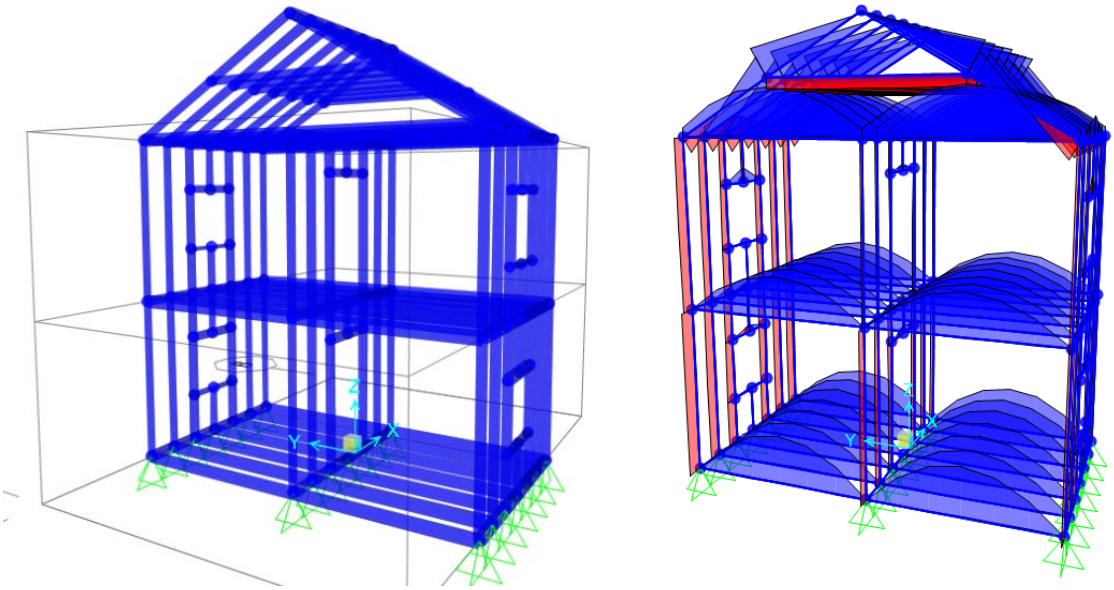

Figure 14 - Condensed Model

A condensed model was created to test the feasibility using of the planar structure to represent the full structure. The joist spans are 16 feet long and the section is 12 feet wide to accommodate the windows and doors. Stress has the tendency of spreading from the point of applied load due to St. Venant's Principle, so it becomes distributed over the tributary width of the area of application as distance increases from the point of the applied load. For this reason, this width was chosen to allow the stress to become uniform towards the edges. The following images show the stress results from the analysis. Quantitative values for the condensed model study can be found in Appendix E - DHS Condensed Model Study.

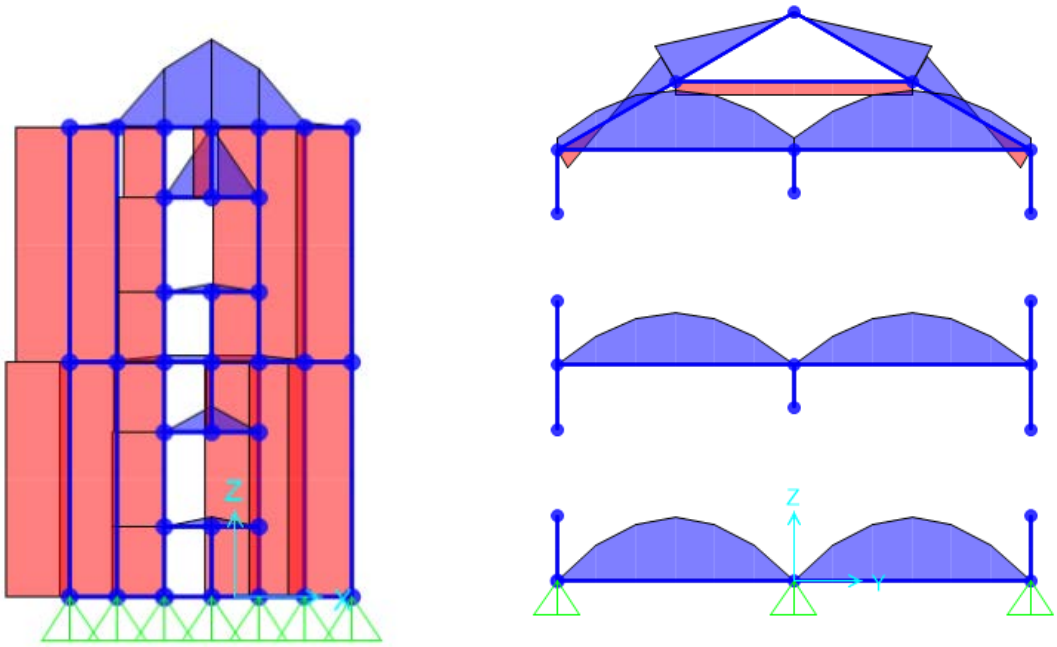

Figure 15 - Stress Results (Condensed Model)

The following figures show the concept of tributary area and how it affects the condensed study. It was desirable to have a smaller section of a full building to serve as the test specimen in the WPI Gateway Fire Lab. For the condensed study, one section of the full building was investigated as indicated by the red box in the figure below. Conventional light, wood-framed construction consists of wood studs placed 16” on center, which creates structural redundancy due to the close spacing of studs. The stress induced by the gravity loads is distributed to the adjacent floor joists and the wall studs. The load is distributed over the tributary area. When referring to the four joists chosen for the condensed model, the tributary area is shown below.

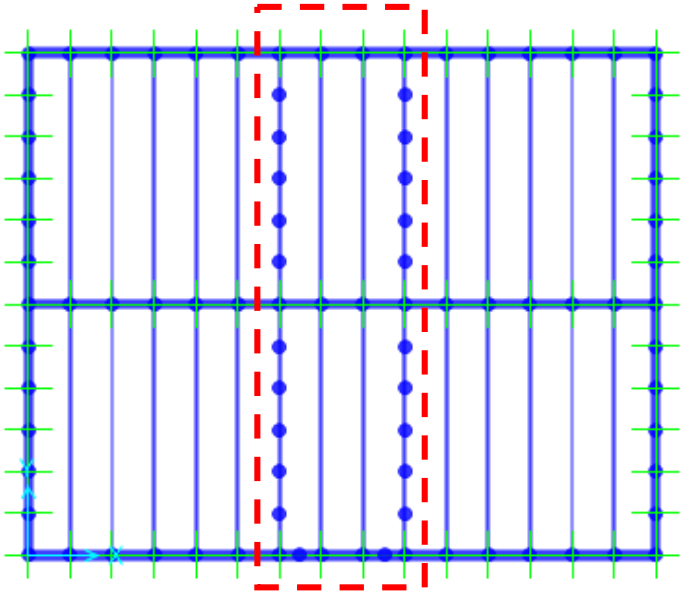

Figure 16 - Tributary Area

The moment and stress results are compared between the full and condensed models. This work was performed for the DHS Green Building Project, and the quantitative results can be found in Appendix E - DHS Condensed Model Study.

2.1.5. Specimen Design Summary

Based on the results from the section analysis, the planar section is an accurate representation of the full residence structure for the static behavior of gravity loads. The stress values for both the joists and studs were very close in both scenarios. The openings for the doors and windows caused concentrations of stress and the studs showed consistent magnitudes of stress along the length of the structure. The quantitative results summary of the DHS Green Building Project condensed study can be found in Appendix E - DHS Condensed Model Study. The test specimen was modeled to exhibit the same stress behavior as the full residence structure.

Regarding dynamic behavior, the full and condensed models would not exhibit the same dynamic response. Structural dynamic behavior depends on the mass, stiffness, and damping of a structure. The condensed model would have less mass due to its decreased size, and it would have less stiffness due to the removal of additional walls and lateral members. The damping is a function of the mass and stiffness. However, the condensed structure created for the DHS Green Building Project was chosen as a low cost way of testing within two different projects. The goals of both this project and their project was combined to create a collaborative effort that would yield useful data for both parties. Although the exact dynamic response of the condensed structure may not represent a full building, the shift in acceleration and frequency due to fire exhibited by the condensed model may be applied to larger structures.

2.2. Test Rig Design

After determining the feasibility of a condensed, planar section model, a test rig was designed to house the test specimens during fire testing. This test rig was designed to accommodate specimens from the traditional, advanced, and structural insulated panel (SIP) configurations for the DHS Green Building Project. Different materials were considered for use in the rig, but the primary focus was initially on aluminum and steel. The goal for the rig is to create a semi-permanent structure that will maintain adequate structural performance for the entire duration of this research project. This means that the structure must be able to endure numerous cycles of high temperature fire testing. The conceptual layout for the test rig is shown below.

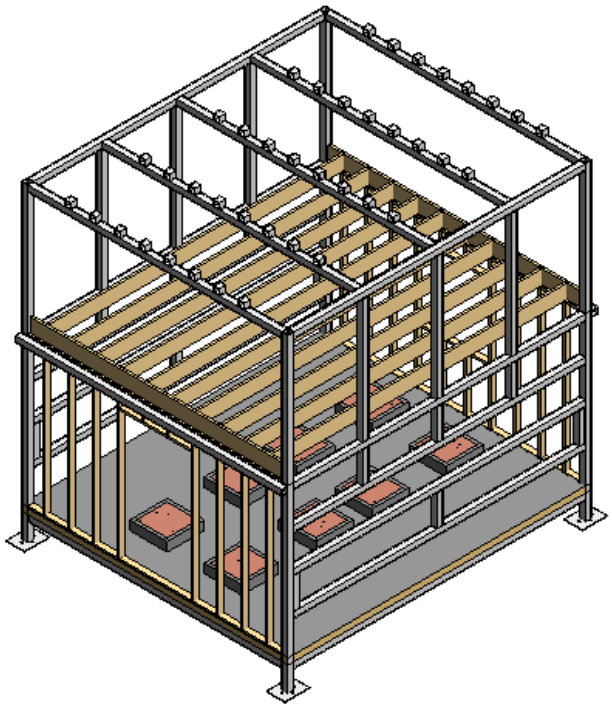

Figure 17 - Test rig (3D view)

The purpose of this design is to provide a sturdy frame in which to house the test specimens. It is designed to accommodate every configuration that will be tested for this project, including the 1st floor and 2nd floor configurations. The test rig is equipped with a moment frame that spans over the test specimen and serves to carry the test loads. In the event of a total collapse of the test specimens, the moment frame would catch the loads and distribute the stress to the steel instead of letting the heavy test loads crash to the floor. This addition required for the test rig design was chosen for feasibility of load application and safety.

The test rig was also designed with vent doors on its lateral sides, opposite of the test specimen walls. Vents are needed to provide the proper amounts oxygen necessary for combustion. The study of the various vent configurations is detailed later in this report. From a structural analysis perspective, the vent doors do not carry any load besides self-weight as they are separated from the test load path. For this reason, they could be fabricated from any material including aluminum for its lightweight applications. These vent doors would need to be removed to install the wood specimens before testing and remove the burnt specimens after testing.

2.2.1. Material Comparison

The test rig had to be designed using a material capable of supporting full-scale residential loads. Initially, steel and aluminum were considered for use within the semi-permanent walls within the test rig. The semi-permanent walls refer to the two walls that are not part of the wood test specimens. Aluminum was a desirable choice as it is lightweight and almost as strong as steel. One manufacturer, called 80/20, specializes in structural slotted aluminum members that are typically used for industrial purposes. These members are light and very easy to assemble. Additionally, the other choice of structural members were hollow structural section (HSS) steel members, which are relatively light weight considering their high structural capacity.

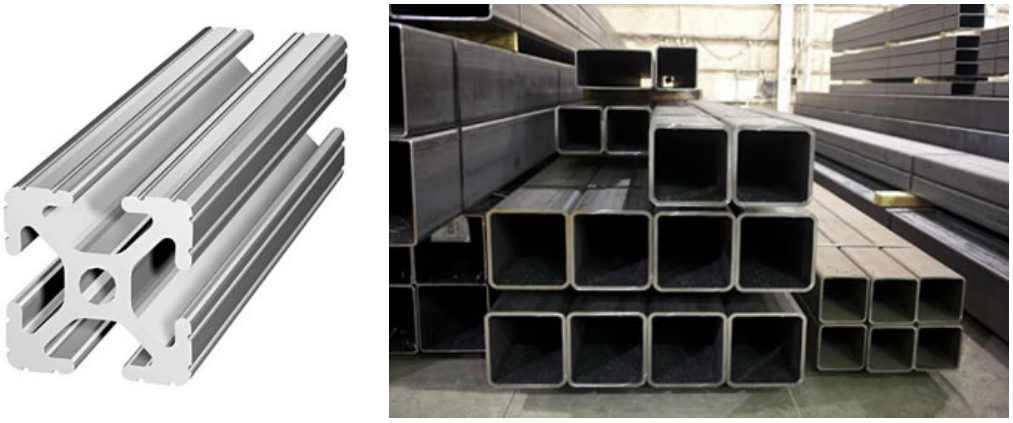

Figure 18 - 80/20 Aluminum and HSS steel Members

However, the biggest disadvantage of using aluminum for this particular project is the poor thermal performance. Comparatively, aluminum has a much higher coefficient of thermal expansion than steel, 13e-06 versus 6.5e-06 in/(in °F) **[21]**. The equation for expansion due to

temperature is shown below. The stress arises when the ends of the members of fixed during thermal expansion.

$$\Delta L = \alpha * \Delta T * L \quad \textbf{Equation 3}$$

$$\epsilon = \frac{\Delta L}{L} \quad \textbf{Equation 4}$$

$$\epsilon = \alpha * \Delta T \quad \textbf{Equation 5}$$

$$E = \frac{\sigma}{\epsilon} \quad \textbf{Equation 6}$$

$$\sigma = \alpha * \Delta T * E \quad \textbf{Equation 7}$$

Where: ΔL = change in length, L = original length, α = coefficient of thermal expansion, ΔT = change in temperature, ε = strain, σ = stress, E = modulus of elasticity

It is important to note that this equation is simplified and assumes fixed end restraints for the derivation of stress. Sometimes structural connections can be designed to provide free expansion of members, and therefore induce less stress. In addition to thermal expansion, material properties can degrade due to elevated temperatures. Yield strength and modulus elasticity are shown to degrade for both steel and aluminum.

Ultimately, steel was chosen as the structural material for the test rig. The steel HSS members offered very high structural capacity and relatively low weight compared to other steel sections. Steel has a much higher performance in regards to yield strength and elastic modulus during fires compared to aluminum, which was the deciding factor for its use in this project.

The figure below shows a comparison between steel and aluminum for the yield strength at elevated temperatures from research performed on cylinders **[22]**. Although that project focused on cylinders, it is an example of the large difference between the structural performance of steel and aluminum at elevated temperatures.

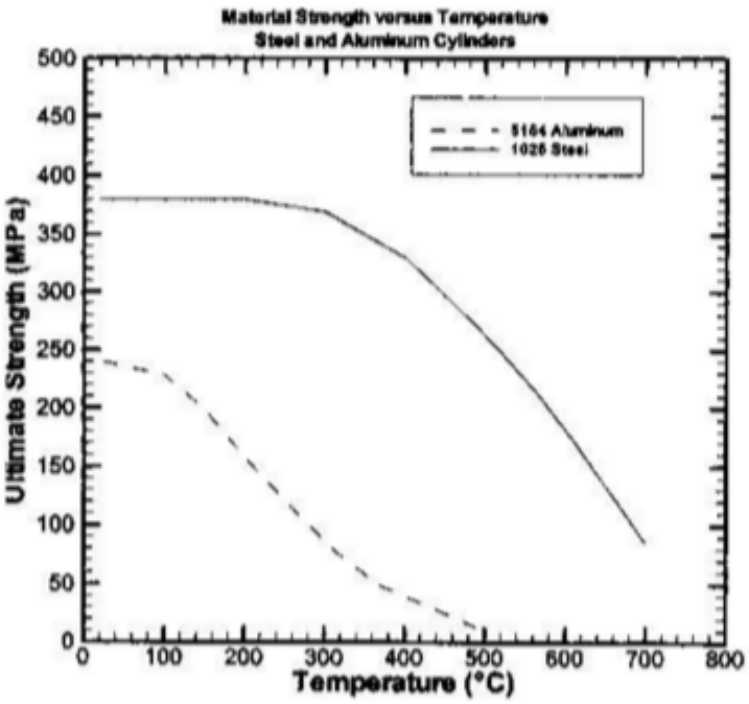

Figure 19 - Yield Strength of Steel and Aluminum

2.2.2. Simple Thermal Analysis

A simple thermal analysis was performed to check the structural performance of the test rig during increased temperatures. This study only investigated the effects of thermal expansion and did not consider the degradation of material properties. It was assumed that adequate insulation could be provided to the steel members to keep the temperature relatively low during fire testing. The yield strength and elastic modulus degrade as temperature increases, which is why the

insulation is needed to keep the temperature of the steel low. Large stress concentrations due to restrained thermal expansion can also occur due to an increase in the temperature of the steel. The model created in SAP2000 was modified to include induced temperatures. The following figure show the stress caused by a uniform increase in temperature.

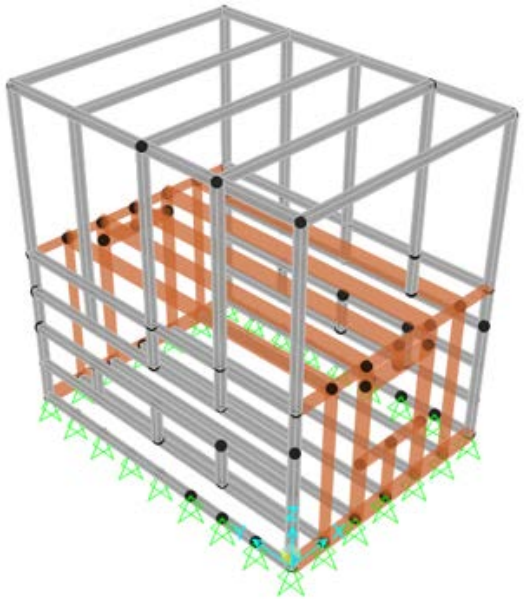

Figure 20 - Simple Thermal Analysis Model

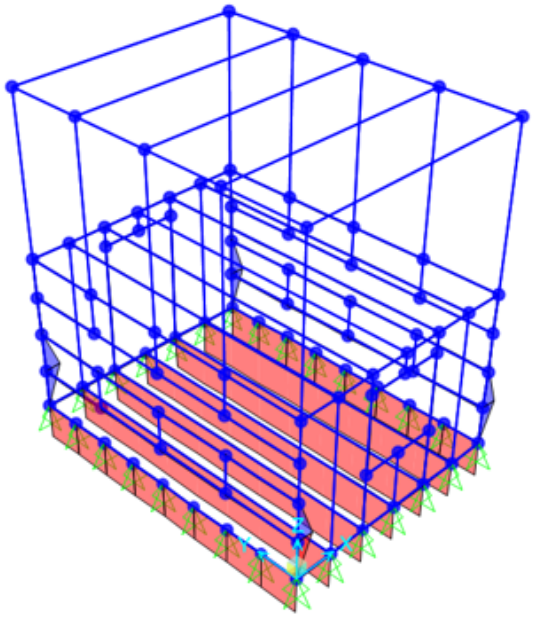

Figure 21 - Simple Thermal Analysis Stress Results

For this simple analysis, the temperature of the entire test rig was increased by 400°F to investigate the stress results. As the results show, there are large concentrations of stress shown by the red in the bottom steel beams used for the floor. This is largely due to the fact that these beams are restrained from lateral displacement by the pin supports shown by green triangles in the figures. After performing this simple thermal analysis, it was clear that the base of the test rig should not be fully restrained, and the steel floor beams should be free to expand to avoid stress by using roller supports. For this reason, the test rig was built upon four caster wheels that act as rollers in the structural analysis model. This also allows the test rig to be moved before or after testing, which is necessary for the use of the WPI Gateway fire lab.

2.2.3. Test Rig Design Summary

In conclusion, steel is the superior choice as the structural material compared to aluminum based on comparison of their structural performance during fires. Steel HSS members can provide a much higher structural capacity than the 80/20 aluminum sections, while still maintaining a relatively low weight. The structural members were designed with the assumption that proper insulation would be provided in order to keep the temperature of the steel as low as possible. In order to keep the steel and aluminum at the same structural capacity, more insulation would be required for the aluminum. The combination of large loads and high temperatures was the reason for choosing steel as the primary structural material for the test rig. This design was necessary for the potential of future testing for the DHS Green Building Project, which could be used to validate the results of this project.

2.3. Fire Modeling Analysis

A fire dynamics model was created using Fire Dynamics Simulator (FDS) to simulate the fire behavior. FDS is a computational fluid dynamics (CFD) model of fire-driven fluid flow. FDS solves numerically a form of the Navier-Stokes equations appropriate for low-speed (Ma < 0.3), thermally-driven flow with an emphasis on smoke and heat transport from fires **[23].** This is a relatively new software tool that allows actual fires to be simulated based upon the physics assumed in the software. It has been primarily used for smoke control systems, automatic sprinkler system design, and fire reconstructions. The model created for this project simplifies the structure as a compartment, which is standard procedure for modeling fires within enclosed areas.

Traditionally, zone modelling has been used to simulate basic compartment fires using the assumption that the compartment is broken into an upper and lower gas layer. In contrast, FDS is a computational fluid dynamics fire simulation that can be used to simulate fires in structures of more complicated geometry. This software was useful to calculate the temperature and heat flux values at specific locations within the test specimen.

The DHS Green Building Project team chose the design fire to create post-flashover conditions exhibited in an actual fire. The suggested temperatures for post-flashover conditions are generally close to 1000°C **[4]**. Through multiple iterations, it was determined that a 4 MW fire provides these conditions. The maximum temperature in the chosen configuration was 1000°C.

These conditions were kept in mind during the detailed thermal analysis to determine specific values of temperature and heat flux within the gas, walls, and ceiling.

The following figure represents the FDS model as depicted in the SmokeView application. SmokeView is a visual tool to display the results of the calculations derived in FDS. The model below uses small slot vents to allow oxygen to flow through the test compartment. The colors represent the temperature within the compartment due to the fire. Specific details of the thermal analysis are elaborated upon in the subsequent chapters.

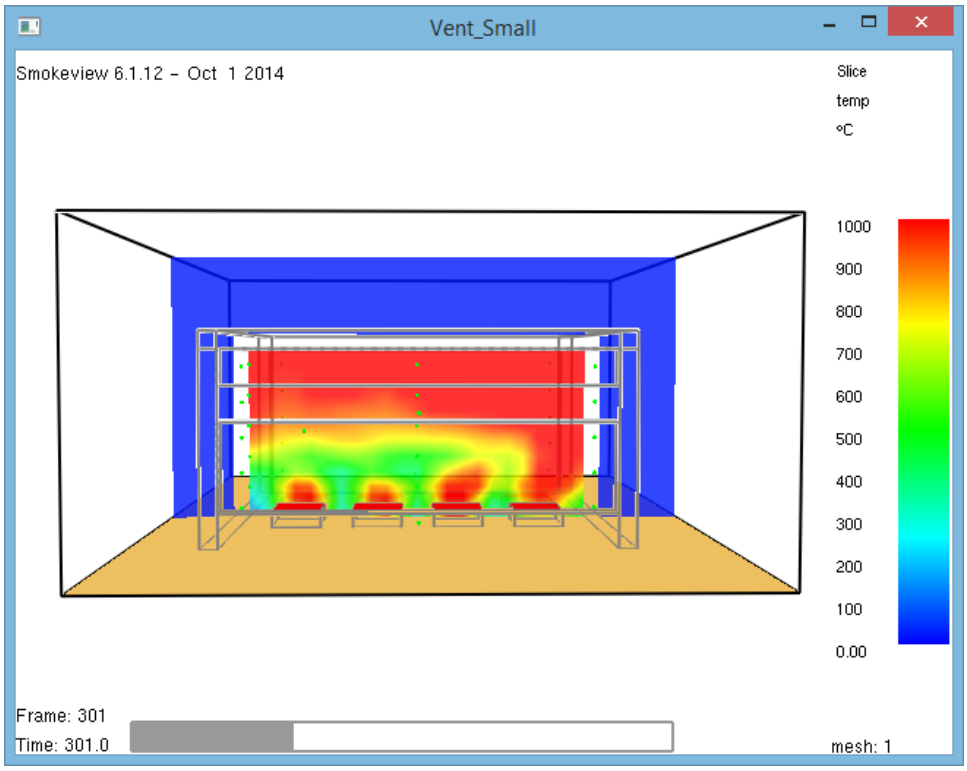

Figure 22 - FDS Model

2.3.1. Burner Configuration

This section details the burner and thermocouple tree configuration used for the simulations. For this project, a 4 MW propane fire was desired to reach post-flashover conditions. Eight burners of 500 kW each were used in the compartment, which equals a total of 4 MW for the entire fire.

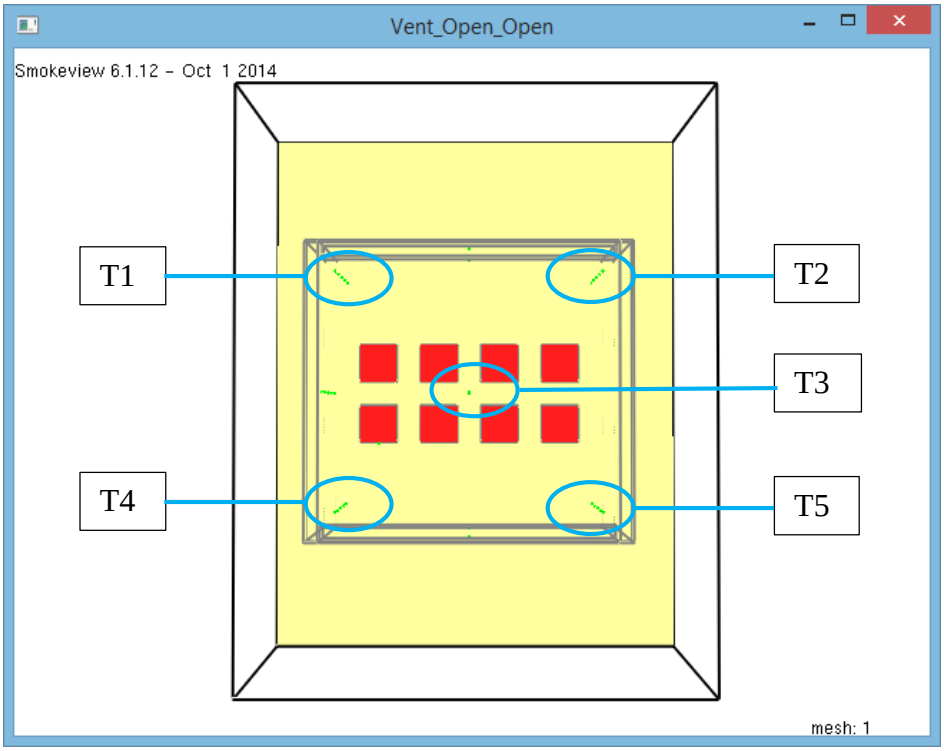

Figure 23 - Burner and Thermocouple Locations

Labels T1 through T5 in Figure 23 represent thermocouple trees and their name designation. Five trees of 5 thermocouples were used for this analysis, each spaced 0.2 m in the vertical direction. This configuration simulates the layout that is currently present in the lab. Thermocouple trees T1, T2, T4, and T5 are located 0.2 m by 0.2 m from each corner of the compartment. Thermocouple tree T3 is located in the center of the compartment.

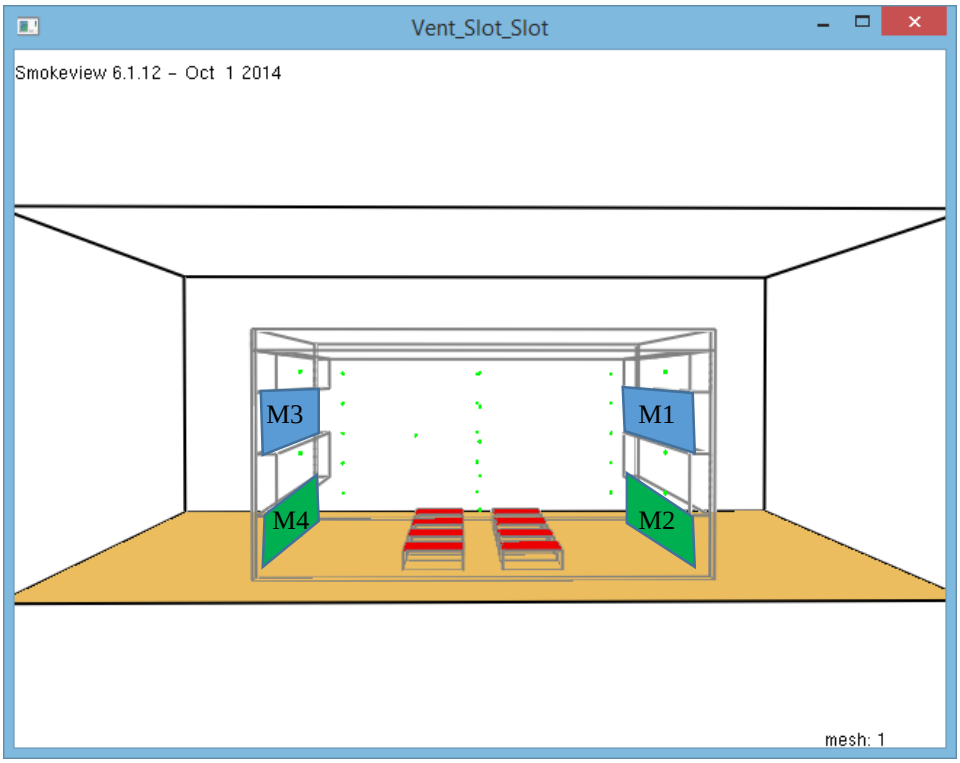

Figure 24 - Burners and Mass Flow Devices

Mass flow rate devices were placed wherever vents were present. The vents were essentially divided in half by designating one vent as the air input and one vent as the air output. The mass flow values were compared against the stoichiometric values to derive the equivalence ratio. This would signify if the compartment in each configuration was fuel rich.

The burners were elevated 6 inches above the floor to more accurately represent the burners used during testing, which rest on the floor instead of being imbedded in the floor. This elevation slightly affects the circulation from vents which can be seen later in this report.

2.3.2. Surface Properties

Six inch Gypsum wallboard was initially used as the surface material for the vent configuration study. This material was used as a simple way to run initial FDS simulations before the actual surface materials were known. The gypsum used has a thermal conductivity of 0.17 W/m*K, a specific heat of 1.09 J/g*K, and a density of 800 kg/m^3. These are typical properties experienced at 300 K. This material was used as the default for all surfaces except for the burners. More specific materials were used once the test specimen was built in the lab.

The following table represents the actual material properties of the surfaces used in the test compartment after it was built. A more specific version of the gypsum insulation is shown after it was chosen by the DHS Green Building Project team. The FDS model was updated to reflect these material properties to have a more accurate depiction of the walls and ceiling. A detailed analysis of the surface temperature profile with this layered surface can be found later in this report.

Table 2 - Material Properties

Material	Dimensions *L x W (ft.)*	Thickness *(in)*	Conductivity *W / mK*	Density *kg / m^3*	Specific Heat *J / kg K*
Sheetrock Type X	4 x 8	0.625	0.258	756	1090
R13 Kraft Insulation	7.75 x 1.25	3.5	0.0388	20.824	795.49
Plywood	4 x 8	0.71875	0.12	545	1215

2.3.3. Vent Configuration Study

The vent configuration study was carried out for the DHS Green Building Project in order to determine the best candidate for the vent configuration. It supplemented this project by supplying a basic FDS model that could be modified for use in the thermal degradation study, which is detailed later in this report.

Five main vent configurations were chosen for this study. The two walls refer to the semi-permanent steel walls that contain the vents. Open means that no divider is present, closed means that the vent is completely closed, and slot means that a divider is present to provide two slot openings. For example: slot open configuration has a slot vent on one wall and an open vent on the other wall.

The following graph shows the average room temperature for each configuration. The average room temperature was calculated by taking the average of the top 3 layers. This would be the average for every thermocouple at 1.2 m, 1.6 m, and 2.0 m above the floor. The temperature values from this analysis were used to evaluate the various vent configurations for use in the DHS Green Building Project test specimen.

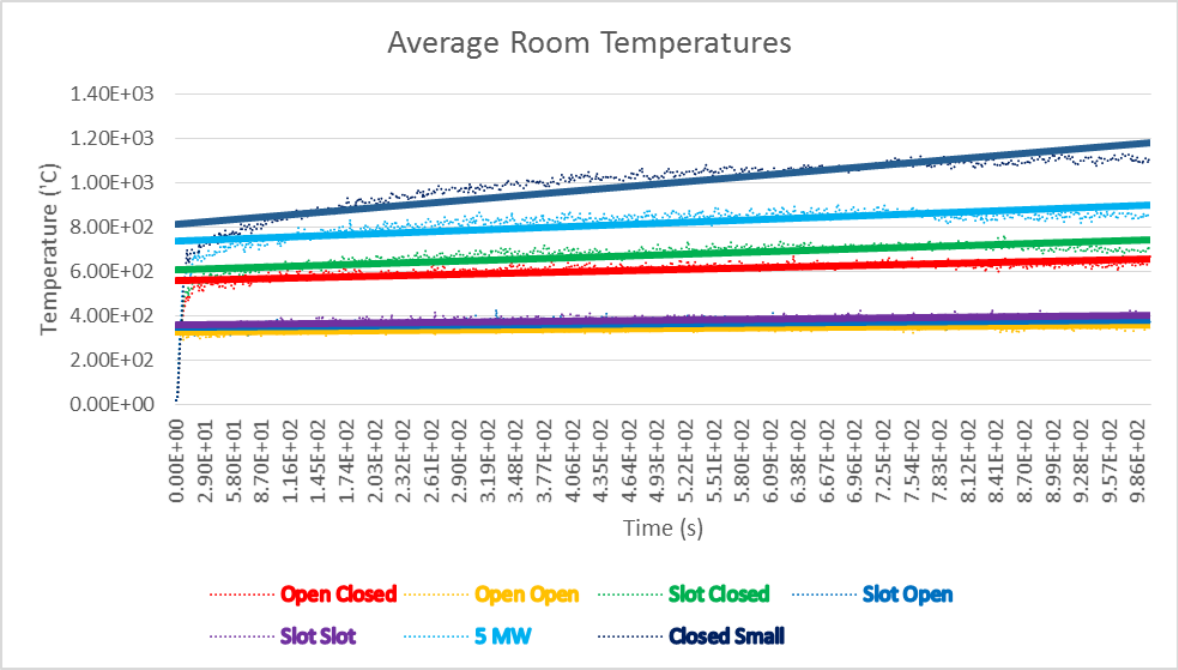

Figure 25 - Vent Configurations Average Temperatures

The average room temperatures for the open open, slot open, and slot slot vent configurations are all close to 400°C. The next configurations in order of rising average temperature are the open closed, slot closed, 5 MW slot closed, and small slot closed vent configurations. The small slot closed configuration has the highest change in temperature over time.

The following table summarizes the findings of the vent configuration study. The four categories for design selection were chosen as symmetric thermal behavior, containment of visible flames, fuel rich state, and average room temperature.

Table 3 - Summary of Vent Configuration Study

Vent Configuration	Symmetric	Flames Contained	Fuel Rich	Avg. Room Temp. (°C)
Open Closed	No	Yes	No	600
Open Open	Yes	Yes	No	400
Slot Closed	No	Yes	No	700
Slot Open	Yes	Yes	No	400
Slot Slot	Yes	Yes	No	400
5 MW Slot Closed	No	Yes	No	900
Small Slot Closed	No	No	No	1100

Based on the results of this study, a few of the vent configurations may be used for testing. Fuel rich state and containment of flames are important factors for both accuracy and safety. The symmetry of temperature, flames, and smoke ensure that all parts of the structure experience the same consistent thermal impact. The average room temperature should be moderately higher than 600°C for post flashover conditions.

It was optimal to choose either the slot closed or the 5 MW slot closed vent configurations. Changing the size of the slot vents seemed to have a large impact on average room temperature. From Table 3, the slot vent configuration provides the best balance between containing flames and keeping a high, symmetric temperature profile. The results of Table 3 were used as a design tool during the selection process of the vent configuration that was used for the actual test compartment built in the WPI Gateway Fire lab.

For this project, the open closed configuration was used because it represents the configuration of the test specimen that was initially built in the WPI Gateway fire lab. The intention was to use a configuration in the FDS model that closely matched the configuration built in the lab so that the results of this research can be validated at a later date by the DHS Green Building Project. The validation of the fire analysis is beyond the scope of this particular project. The vent configuration used for the analysis model is confirmed as the open closed configuration for all sections of this report. The following sections detail the FDS analysis that was performed to investigate the temperature and heat flux profiles for the test compartment.

2.3.4. FDS Model Results

This section details the temperature and heat flux values obtained from FDS for the model test configuration. As previously stated, the open closed vent configuration was chosen as the candidate model for this project as it was most convenient for the application to the DHS Green Building Project. The light, wood-framed test specimen that was initially built in the WPI Gateway Fire Lab will ultimately be used for preliminary testing, such as temperature profiles, heat flux, smoke propagation, and device calibration for the convergence meter and accelerometers. The following assumptions were made:

- 4 MW propane fire at 1000 second test
- 8 burners at 0.5 MW each
- 16’ by 14’ by 8’ compartment
- 6” gypsum wallboard for walls and ceiling
- Open-Closed vent: one vent completely open, one vent completely closed

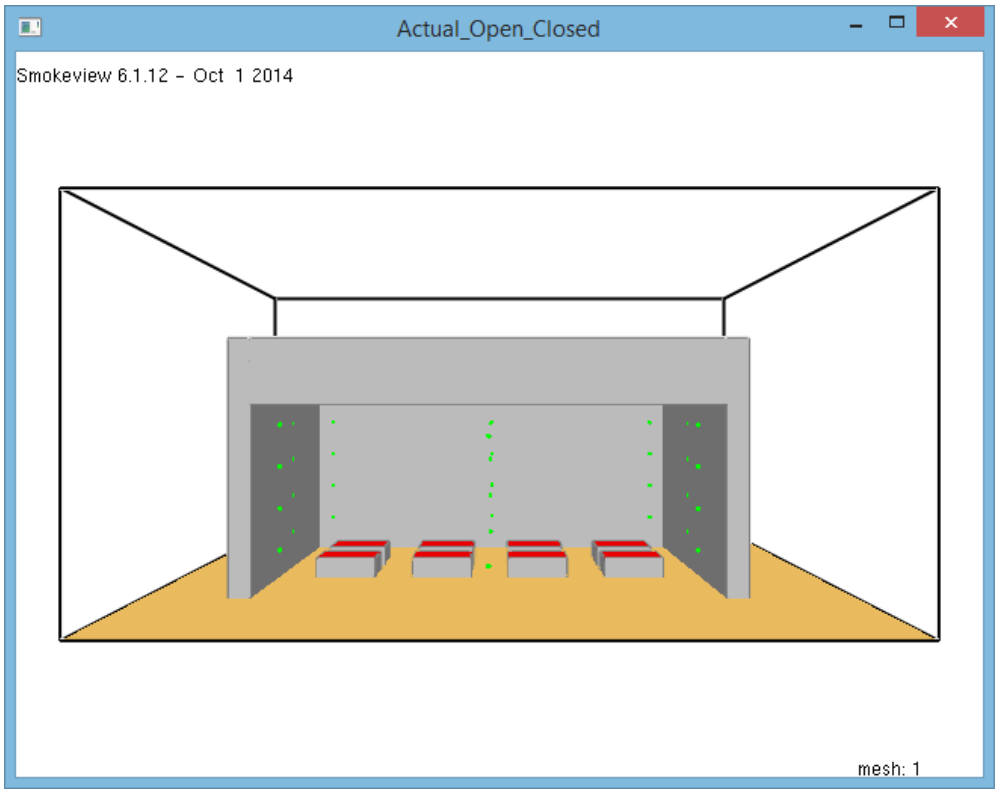

Figure 26 - Chosen FDS Model

The figure above shows test compartment for the chosen vent configuration as it appears in the SmokeView application. SmokeView is useful for showing visual data such as planar gas temperature profiles within the compartment. The elevated burners are shown with the red surfaces, as well as point devices for temperature and heat flux that are represented by the green dots. The computational domain was extended beyond the test specimen to capture data on the smoke plume and temperature outside of the vent. Referring to Figure 23, each location is a temperature tree consisting of 5 thermocouples spaced 0.4 meters apart from the floor to the ceiling. This allows the temperature profile to be broken up according to temperature tree location or by device layer height location.

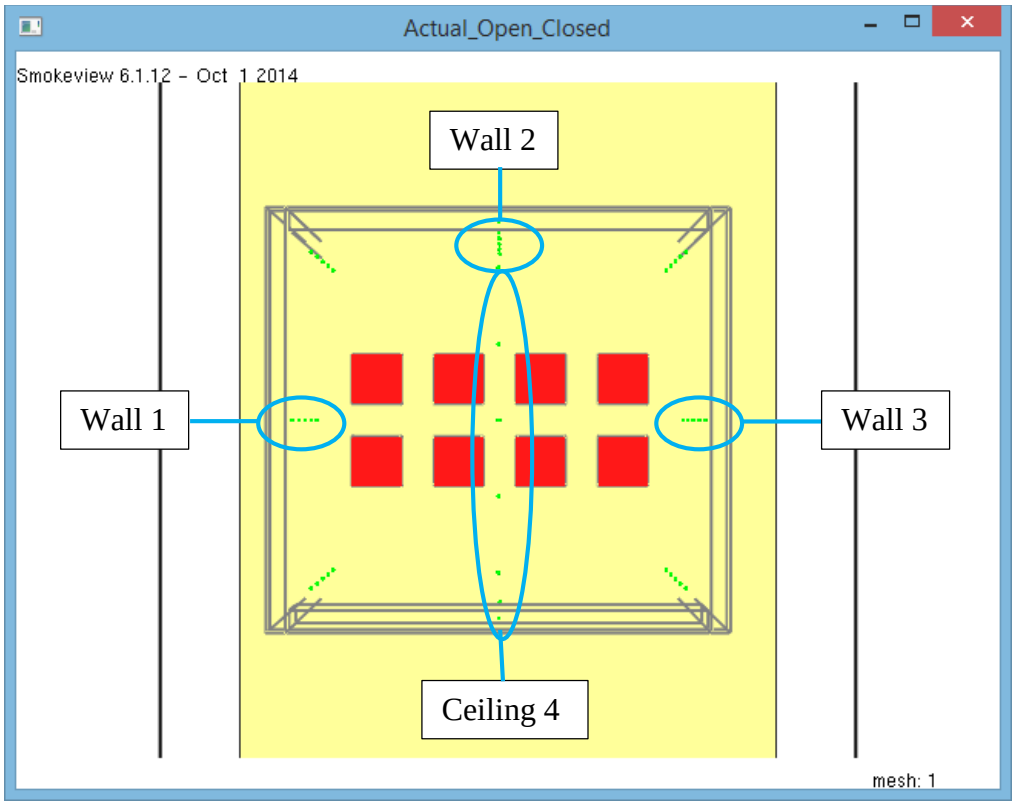

Figure 27 - Heat Flux Device Locations

The figure above shows the locations of the point heat flux devices used in the test compartment. Net heat flux and incident heat flux were measured at the centers of the 3 walls and the ceiling. Five point devices were set at each of the 4 locations to investigate the differences in position. The heat flux did not drastically vary along the height of the wall, but it was still useful to investigate the variations between the three specimen walls and the ceiling.

The following results show the average values collected by the point temperature and heat flux devices within the FDS model. An Excel sheet was created to interpret the data exported from FDS by calculating the average values as specific locations.

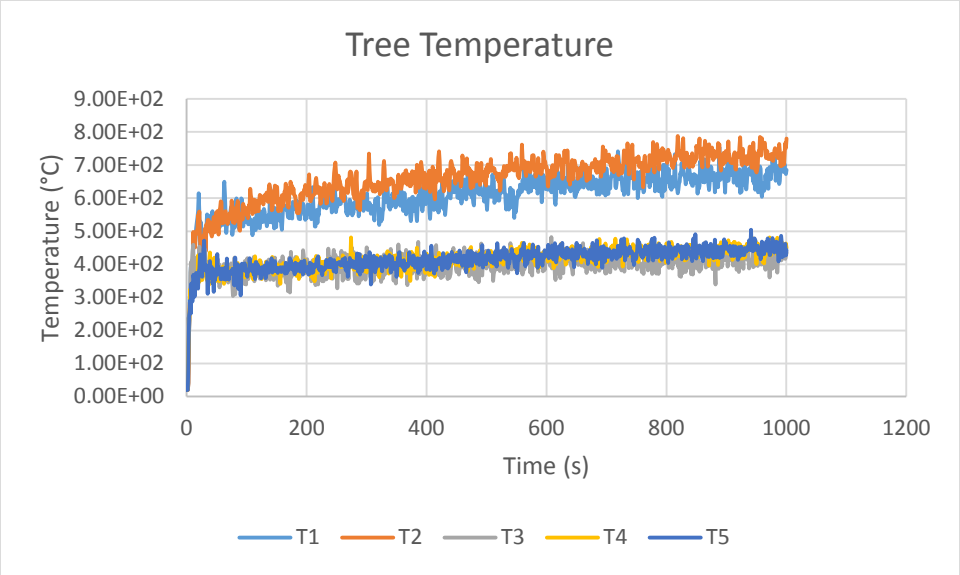

Figure 28 - Tree Temperature Graph

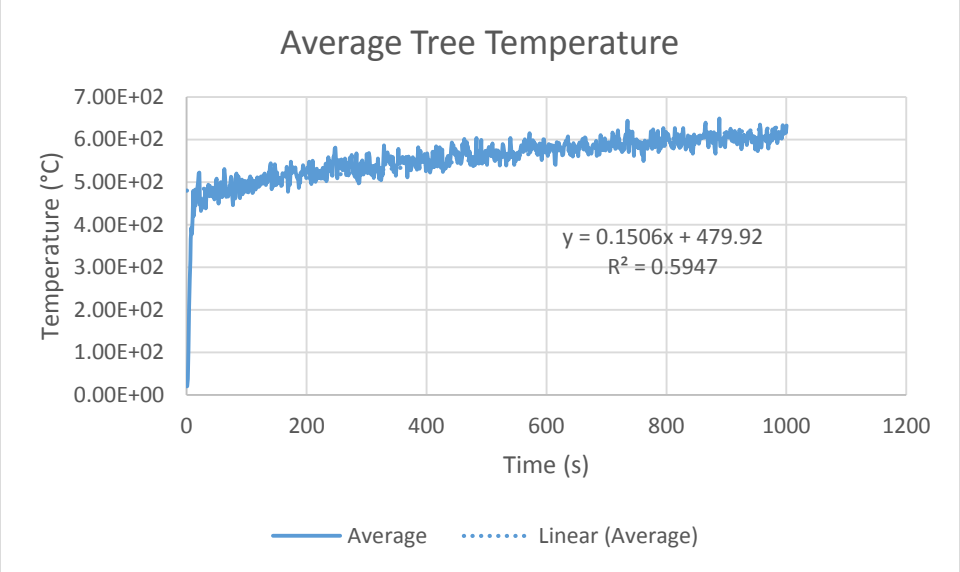

Figure 29 - Average Tree Temperature Graph

These graphs show the average temperature values for each temperature tree. This is calculated by taking the average of all 5 devices along the height of a particular tree location. This provides a temperature profile for the XY-plane of the test compartment. Figure 29 shows the average temperature of all 5 trees. The line of best fit equation is provided in the average graph.

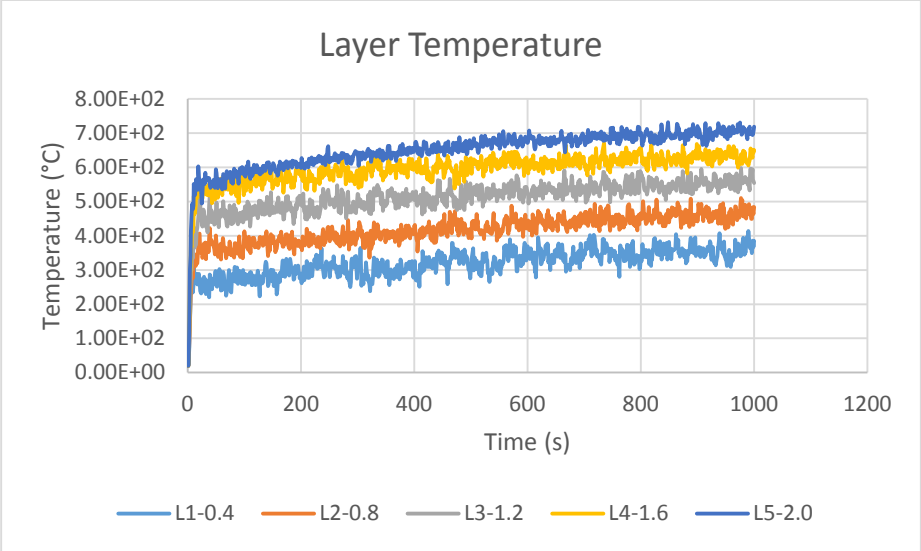

Figure 30 - Layer Temperature Graph

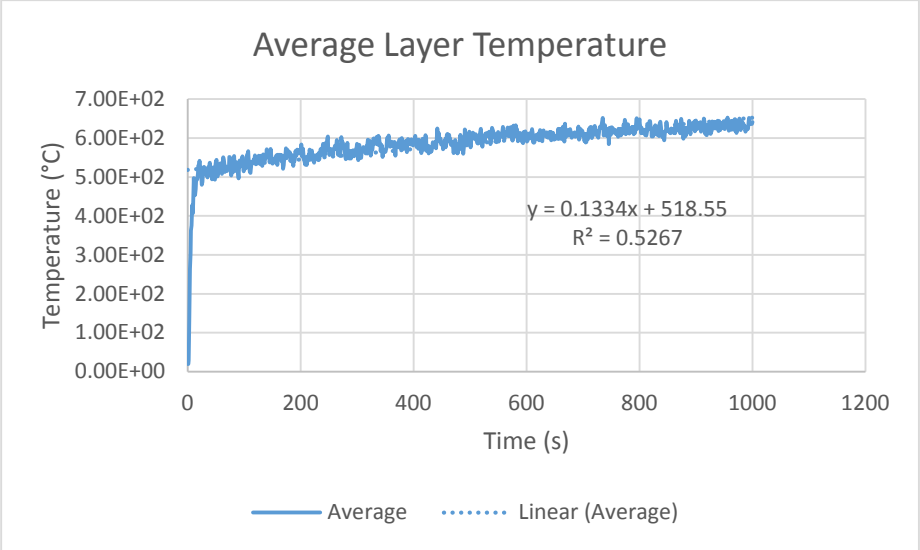

Figure 31 - Average Layer Temperature Graph

These figures show the average temperature values for each layer along the height of the test compartment. This is calculated by taking the average of every point device along a particular layer height (0.4 m). This provides a temperature profile along the XZ/YZ-planes of the test compartment. Figure 31 shows the average temperature of all 5 layers. The best line of fit equation is provided in the average graph.

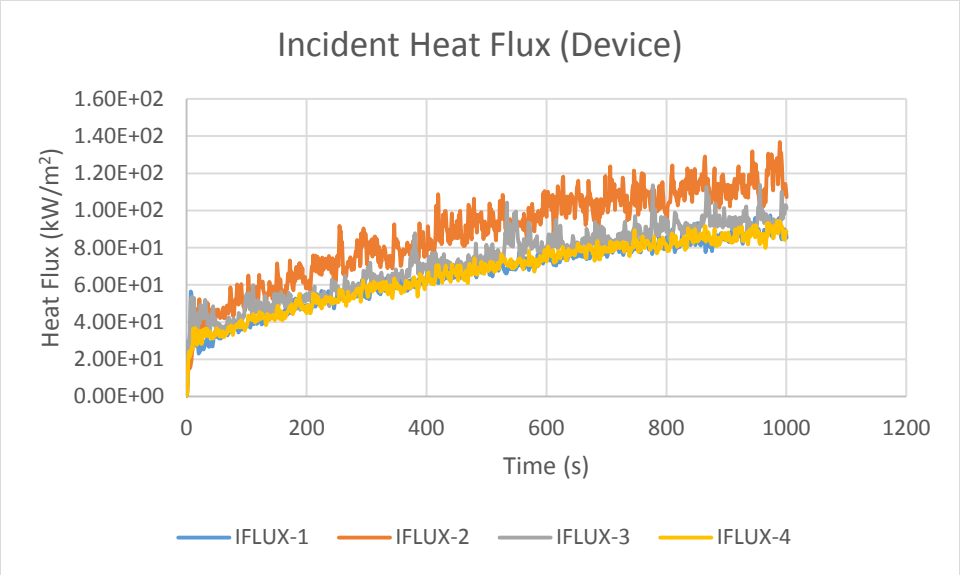

Figure 32 - Incident Heat Flux Graph

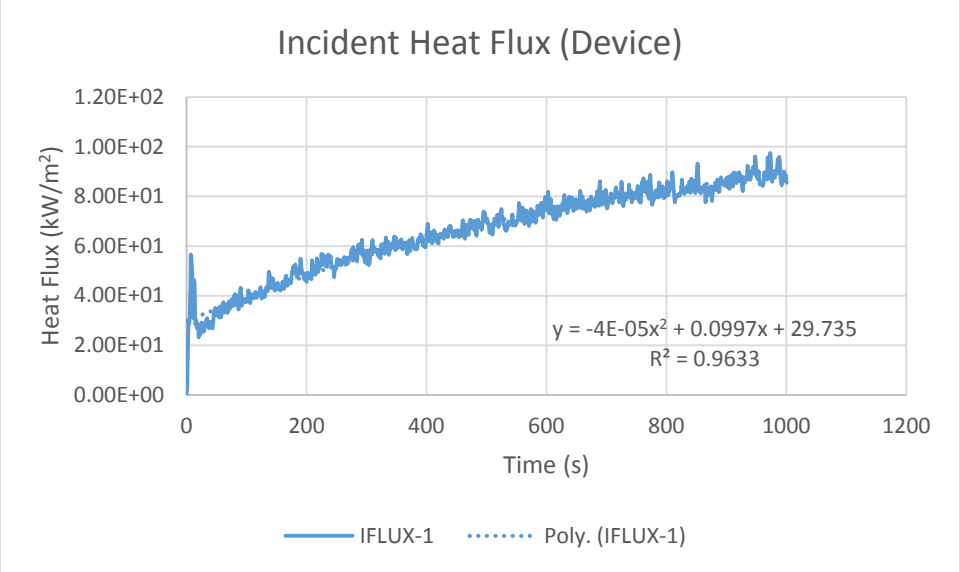

Figure 33 - Incident Heat Flux Graph (Wall 1)

These figures depict the incident heat flux induced upon the system at the various locations within the test compartment. All units for heat flux are reported in kW/m^2. The incident heat flux for Wall 1 ranged from 20 to 70 kW/m^2. This data was used to calculate the char rate, which is detailed later in this report.

2.3.5. Model Surface Temperature Profiles

This section provides a more detailed analysis of the walls and ceilings of the test specimen. The previous sections assumed the surfaces were made completely of gypsum, whereas this section uses layered surfaces. The following graphs represent the surface temperature profiles generated by the Actual Test Configuration FDS simulation. Profiles were generated at the center of each wall and the center of the ceiling.

In typical wall framing, the wood studs are supplemented with insulation to retain the heat within a house. Gypsum insulation is provided on the interior face of the walls and ceilings to provide a fire resistance rating, which is determined by the type and thickness of the particular insulation material.

The following figure represents a wall assembly as depicted in UL Design Guide U349 **[10]**. The ratings assume that the wall is exposed to fire only on the interior face. This particular design guide is for a bearing wall rating of 2 hours and a stud with finish rating of 55 minutes. Specific fire resistance ratings can be determined using ANSI/UL 263, which has a section for wall assemblies **[10]**.

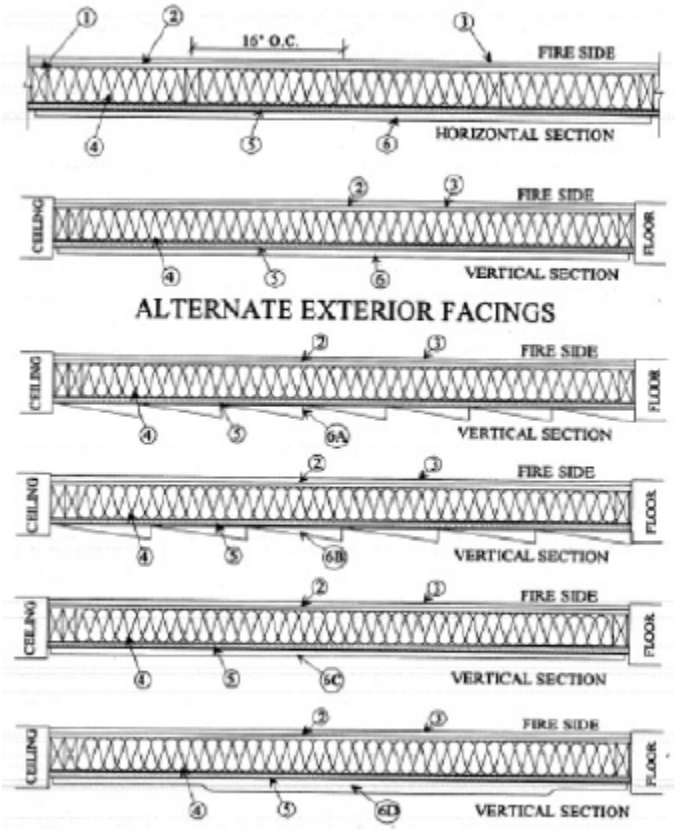

Figure 34 - U349 Wall Assemblies

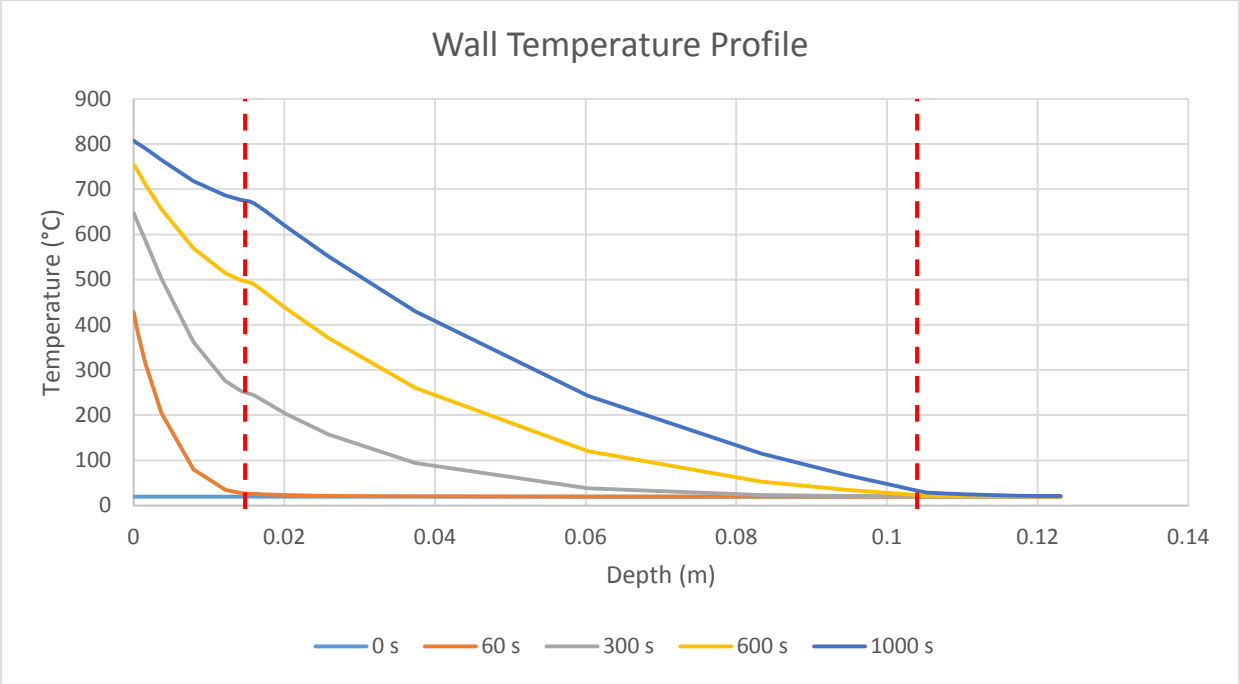

Figure 35 - Wall Temperature Profile Graph

The graph above represents the temperature profile predicted by the FDS model for the wall within the test configuration. The size of the wall studs are a nominal 2” x 4”. The red dotted lines represent the material interface zones between the different material layers. The x-axis represents the depth within the wall, and the y-axis represents the temperature in degrees Celsius. The rate of temperature change varies as the material layer changes. The maximum temperature at the surface is approximately 800°C, and the temperature gradient of the interior cavity that contains the studs varies from 50°C to 700°C at the end of the simulation.

Similar to Figure 35, the figure below shows the predicted surface temperature profile within the ceiling of the test configuration. It follows the same behavior as the wall temperature profile, but the ceiling is almost twice the thickness. The graph shows that the heat does not fully penetrate the entire thickness of the ceiling, and the surface that is not exposed to the fire remains close to 20°C at the end of the simulation. The size of the floor joists are a nominal 2”x10”.

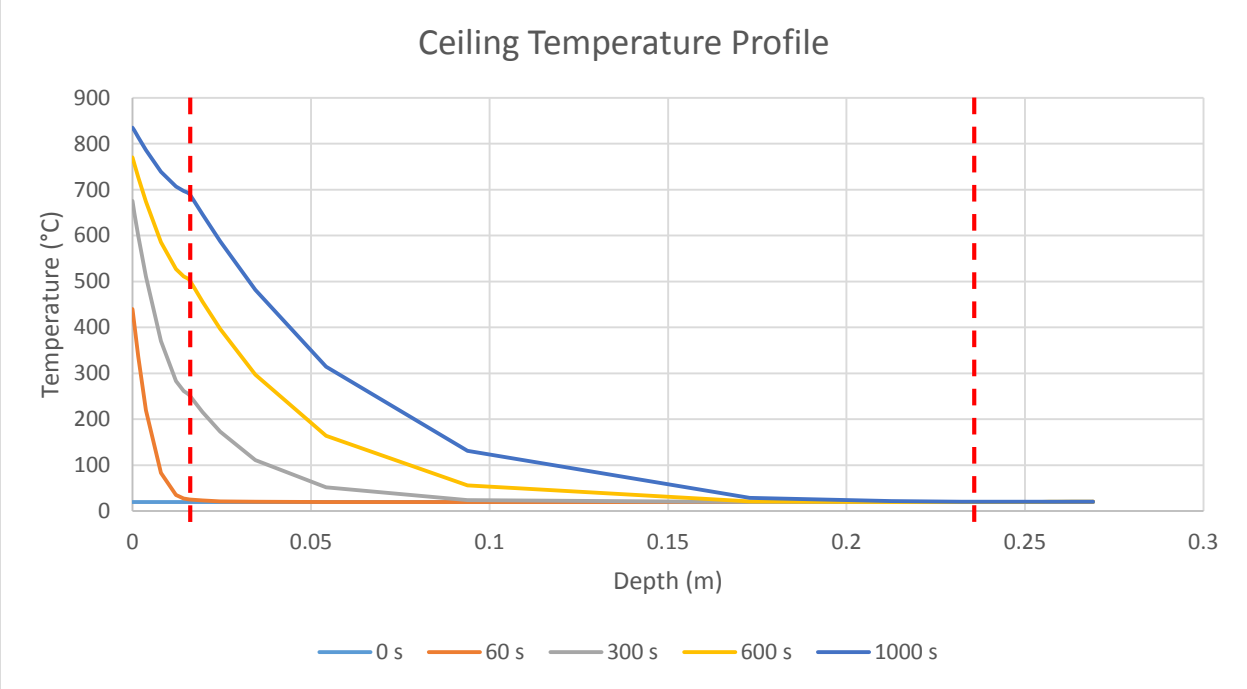

Figure 36 - Ceiling Temperature Profile Graph

Both temperature profiles exhibit similar behavior in various layers. The temperature rises significantly quickly in the first layer of sheetrock and much slowly within the inner cavity containing the studs with insulation for both the walls and ceiling. Through this method, the temperature at specific depths within the walls or ceiling can be estimated through FDS.

2.4. Reduction Theory

The purpose of this section is to introduce the concept of reduction theory, which is the reduction of structural properties and its effect on structural dynamic matrices. Regarding materials, wood members lose cross-sectional area during fires due to charring. The effective char rate decreases over time due to the formation of the char layer, which serves as a natural layer of insulation. The nominal char rate is assumed to be 1.5 in/hr and is used to calculate the effective char rate **[13]**.

$$\beta_{eff} = \frac{1.2\beta_n}{t^{0.187}} \qquad \textbf{Equation 8}$$

Where: $\beta_{eff} =$ effective char rate (in/hr), $\beta_n =$ nominal char rate (1.5 in/hr), $t =$ exposure time to E119 (hr)

This equation assumes exposure time in a standard E119 fire and is based upon timber construction, which has members much larger than light, wood-framed construction. Recent experiments using cone calorimeters have yielded the following equation **[14]**.

$$\beta_{eff} = 0.23(\dot{q}''_{tot})^{0.5} t^{-0.3} \qquad \textbf{Equation 9}$$

Where: $\dot{q}''_{tot} =$ external heat flux (kW/m^2), t = exposure time (min)

This equation is more relevant as it more accurately depicts the scenario used for this project. The incident heat flux varies over the duration of the simulation, so the effective char rate

becomes time dependent. The heat flux values were calculated using FDS and extracted to Excel in order to calculate the new, reduced member dimensions at each time step.

All structures utilize mass, damping, and stiffness to resist dynamic forces. The equation for stiffness is shown below and is affected by the elastic modulus, moment of inertia, and member length. This equation refers to a simply supported column, but it is shown to show the relationship between elastic modulus, moment of inertia, and stiffness. As the moment of inertia degrades due to the loss of cross sectional area caused by charring, the structural stiffness is reduced. The elastic modulus is also degraded due to temperature and further reduces the structural stiffness. This means that the stiffness of the system becomes time dependent based on the char rate and heat flux.

$$K = \frac{P}{\Delta} = \frac{48EI}{L^4} \qquad \textbf{Equation 10}$$

Where: K = stiffness, P = load, Δ = displacement, E = modulus of elasticity, I = moment of inertia, L = length

$$I_x(t) = \frac{(b - \beta t)(h - \beta t)^3}{12} \qquad \textbf{Equation 11}$$

Where: I_x = moment of inertia (in^4), t = time (sec), b = width (in), h = height (in), β = char rate (in/sec)

It should be noted that Equation 11 used for char rate is based upon the total external heat flux, which is assumed to be the incident heat flux for this study. A more accurate method would be to find the total heat flux through the interface of the gypsum insulation. The tests that were performed to derive Equation 11 assumed the wood members were directly exposed to fire, which is not the case for this project. In this case, it can be assumed that the gypsum insulation would provide additional time before the ignitions temperature of the wood is reached.

The char rate is assumed to affect only the sides of the structural members that are closest to fire-exposed face of the walls. For this project, the char rate was assumed to be 100% for the side of the studs closest to the fire and 50% for the lateral sides that are in contact with the thermal insulation material.

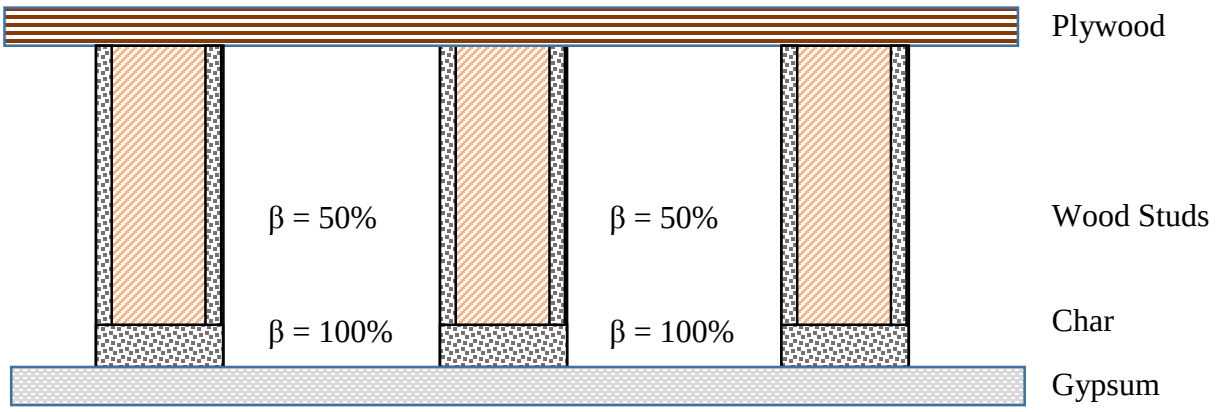

Figure 37 - Char Rate Diagram

If the assumed char rate is 50% for the lateral sides of the wood members for two sides, then the effective char rate would essentially be equal to 100% for the width dimension of the members.

The char rate for the side exposed to the fire would also be 100%, but it would not affect the side opposite of the side exposed to fire. Therefore, the effective char rate would be 100% for both the width and height dimensions of the wood members.

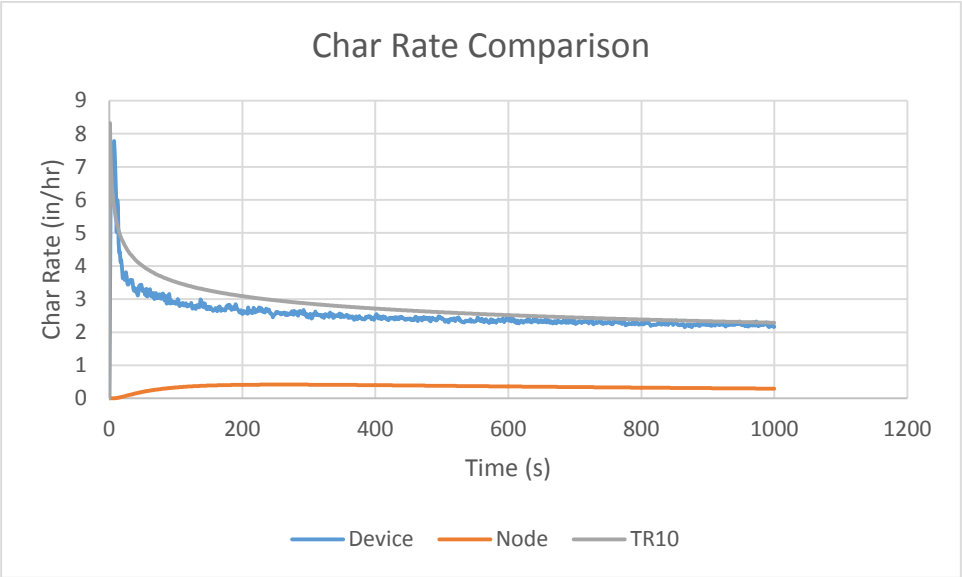

Figure 38 - Char Rate Graph

This graph represents the effective char rate as a function of time measured in inches per hour. The char rate was compared between the incident heat flux device, the hand calculation from the temperature profile, and TR10 values. The node hand calculations using the temperature profile was an attempt to understand the char rate due to the net heat flux at the interface of the gypsum and the studs. However, this data set was not used as it was not representative of accepted values used by TR10. The values from the incident heat flux devices were used instead. The fire that was used in the FDS simulation was set to reach its peak heat release rate of 4 MW within 3 seconds, which is the default ramp function of FDS. This growth rate is not representative of real fires, but it can still be used to understand the behavior of this theoretical model.

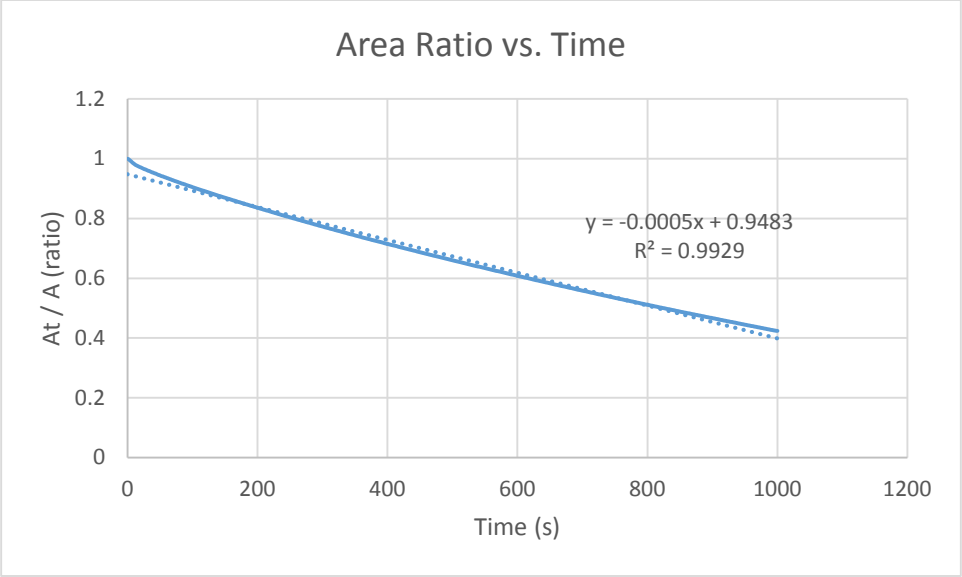

Figure 39 - Area Ratio Graph

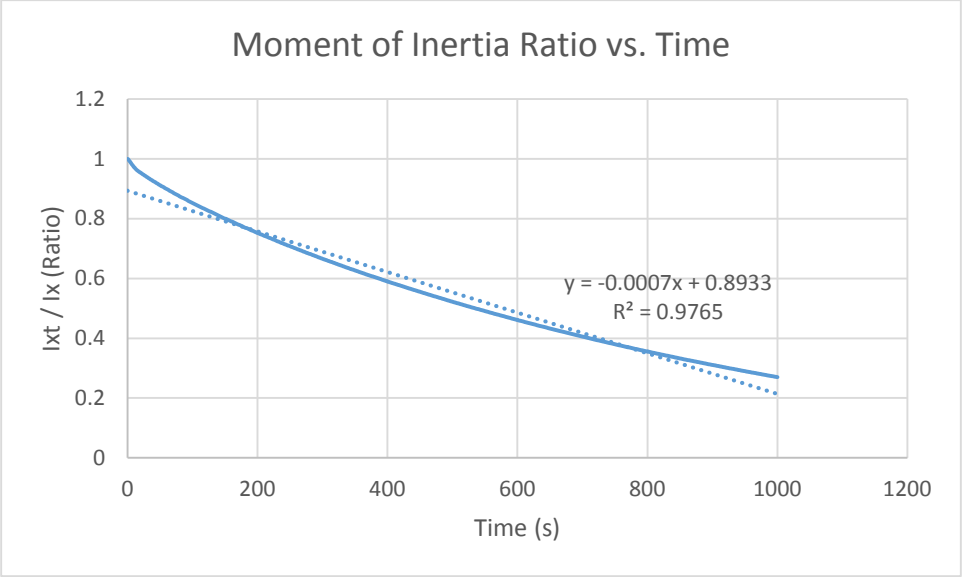

Figure 40 - Moment of Inertia Ratio Graph

These graphs represent the ratios of the moment of inertia and area due to charring, which refers to the ratio of the temperature affected value divided by the original value. The moment of inertia ratio was used to adjust the stiffness matrix, and the area ratio was used to adjust the mass matrix.

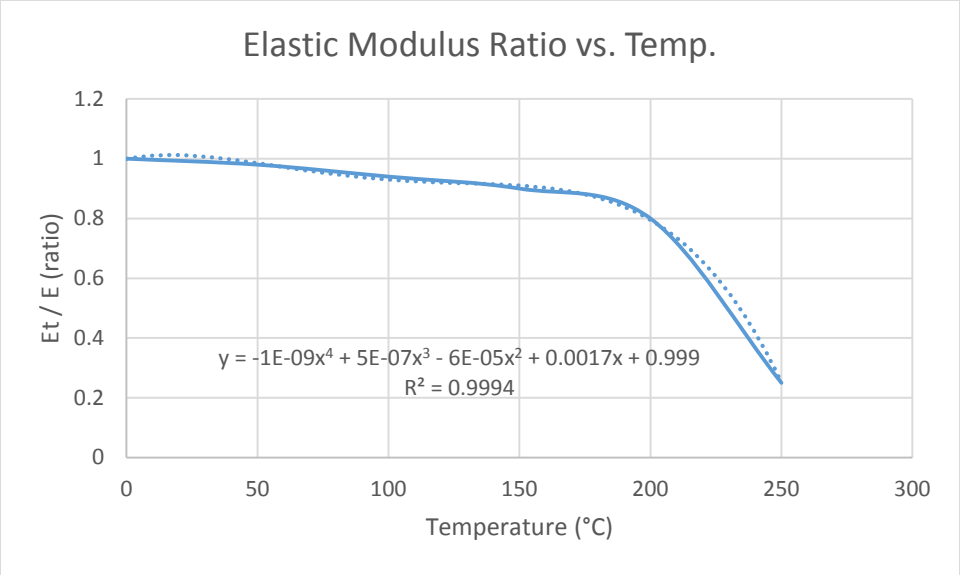

Figure 41 - Elastic Modulus Ratio Graph

The graph above shows the elastic modulus ratio of wood as a function of time. This is equal to the temperature-affected elastic modulus divided by the original elastic modulus. Although the elastic modulus of a material has a large impact on the stiffness matrix, it was not used for this project due to limited available of information. It is shown in the graph that the elastic modulus of wood drops to 30% of the original value at only 250°C. Temperatures above this value would ignite the wood and cause it to char. For this project, the internal cores of the wood members were assumed to be unaffected by the fire. Instead, the focus was the degradation of geometry due to the charring effect of wood. The only factor that affects the degradation of stiffness is the moment of inertia for this project.

After the area and moment of inertia ratios were calculated in Excel, the equations of the lines of best fit for the graphs were exported to Matlab to be used in the dynamic model. The equation of the moment of inertia ratio was used to derive the stiffness matrix reduction factor. The area ratio

was used to derive the mass matrix reduction factor. The mass of each wood member was assumed to be directly related to the loss of cross-sectional area. In reality, the density of the members also degrades due to temperature. This behavior is still an active area of research, and the data for southern pine was not readily available. For that reason, the effect of degrading density was excluded from the scope of investigation. The following equations represent the reduction factors for the mass and stiffness matrices.

$$M_t = R_A * M \quad \textbf{Equation 12}$$

$$K_t = R_I * K \quad \textbf{Equation 13}$$

Where: M_t = temperature adjusted mass matrix, M = mass matrix, R_A = area ratio, K_t = temperature adjusted stiffness matrix, K = stiffness matrix, R_I = moment of inertia ratio

A time of 1000 seconds was used to test the degradation of the end of the simulation, as this time period was the total time of the FDS simulation. The incident heat flux values were used from FDS to calculate the char rate as a function of time, which was used to calculate the reduction factors.

The following table represents the reduction factors that were used in this project. The reduction factors for the mass matrix and the stiffness matrix were not the same, which affects the frequency of the structural dynamic response. This is discussed in more detail later in the report.

Table 4 - Matrix Reduction Factors (t = 1000 s)

	Reduction Factor
Mass Matrix	0.4483
Stiffness Matrix	0.1933

It should be noted that the damping matrix could also be reduced if enough information was known. The initial damping matrix was derived using the Rayleigh method using the initial mass and stiffness ratios. The damping ratio used to create the damping matrix affects the frequency of the structural dynamic response, so this could be a possible source of error during testing. The influence of temperature on the damping ratio was excluded from the scope of investigation for this project due to the lack of available data.

3. Results

This chapter outlines the dynamic analysis model that was created for this project. It provides detail on each of the Matlab scripts that were used to create the model. Each component detailed in previous chapters made a contribution to the creation of the dynamic model.

3.1. Dynamic Model

Matlab was the primary tool that was used to create the dynamic model. This model was designed to accept any combination of mass, damping, and stiffness matrices. The mass and stiffness matrices were extracted from SAP2000 using Matlab.

The state-space equation is used to derive the dynamic response of the structure. It calculates the displacement, velocity, and acceleration response based on the input structural matrices and input force. The acceleration response was the focus of this project. The following equations depict the state space equation.

$$\dot{x} = Ax + Bu \qquad \textbf{Equation 14}$$

$$y = Cx + Du \qquad \textbf{Equation 15}$$

Where: A = system matrix, B = input matrix, C = output matrix, D = feedthrough matrix (0), x = states, $\dot{x}$ = state derivative, u = input, y = output

The state-space equation is useful when dealing with massive systems, such as high-rise structures. The matrices can be manipulated to yield a certain desirable result, which was acceleration in this case. Matlab simplifies the process of creating the A, B, C, and D matrices

that are required to use this equation, which is part of the reason the software was chosen for this project.

First, the dynamic analysis code uses the mass, damping, and stiffness matrices derived in the "Matrix Extract" script to create the state-space matrices (A, B, C, and D) that are required for the state-space equation. It then extracts theoretical input force data from a modal hammer that was used simply to collect an impact force. The following equations present the matrices that are used in the state-space equation.

$$A = \begin{bmatrix} 0 & I \\ -KM^{-1} & -CM^{-1} \end{bmatrix} \quad \textbf{Equation 16}$$

$$B = \begin{bmatrix} 0 \\ M^{-1} \end{bmatrix} \quad \textbf{Equation 17}$$

$$C = \begin{bmatrix} I & 0 \\ 0 & I \\ -KM^{-1} & -CM^{-1} \end{bmatrix} \quad \textbf{Equation 18}$$

$$D = \begin{bmatrix} 0 \\ 0 \\ M^{-1} \end{bmatrix} \quad \textbf{Equation 19}$$

The damping matrix was created using the Rayleigh damping method outlined by Chopra **[24]**. A damping ratio of 5% was used for the first and second modes. The Rayleigh method is based upon the initial mass and stiffness matrices, so the damping ratio values chosen determine the accuracy of the simulations. An iterative process was used to choose the most accurate damping ratio value. The value of 5% was chosen as a smaller, conservative value to use for the theoretical dynamic model. Chopra suggests using a damping ratio of 15% for 1-2 story light, wood-framed structures **[24]**, but the structure used for this project is much smaller than a full-sized building. This was varied in conjunction with the mass and stiffness matrices to more accurately reflect a smaller sized structure.

The following equations represent the Rayleigh Damping Method. Note that the scalars can be calculated with one damping coefficient when both modes are assumed to have the same damping.

$$C = a_0 M + a_1 K \quad \textbf{Equation 20}$$

$$a_0 = \xi \frac{2 w_i w_j}{w_i + w_j} \quad \textbf{Equation 21}$$

$$a_1 = \xi \frac{2}{w_i + w_j} \quad \textbf{Equation 22}$$

Where: M = mass matrix, C = damping matrix, K = stiffness matrix, α_0 = scalar 1, α_1 = scalar 2, w_i = natural frequency of 1st mode, w_j = natural frequency of 2nd mode, ξ = damping coefficient

Then, the code applies the matrix reduction factors calculated in the reduction Excel sheet to Matlab. The mass and stiffness matrices are reduced using the reduction factors mentioned previously in this report. The same reduction factor was applied to every element within the matrices of the structure. In reality, a fire would be non-uniform and would have higher concentrations of temperature and heat flux in specific locations throughout a structure. However, this project assumes a uniform temperature and heat flux profile for the entire test compartment, so every element is assumed to undergo the same reduction.

Next, the code continues the “Simulink Analysis” script using the state space equation to produce two sets of output data, one for the period before the fire and one for the period after the

fire. This output data contains the displacement, velocity, and acceleration response of the structure. A simulation time is calculated to match the time that was given with the theoretical modal hammer impact force. It extracts the output data from Simulink and creates matrices for the displacement, velocity, and acceleration responses of the structure. The maximum values for each element are graphed to facilitate comparisons of the periods before and after the fire. Separate files were created for displacement, velocity, and acceleration responses to reduce file sizes. As acceleration is the means of comparison from the data collected from modal testing, the acceleration response files were used for this project. The figure below depicts the Simulink model used for this project.

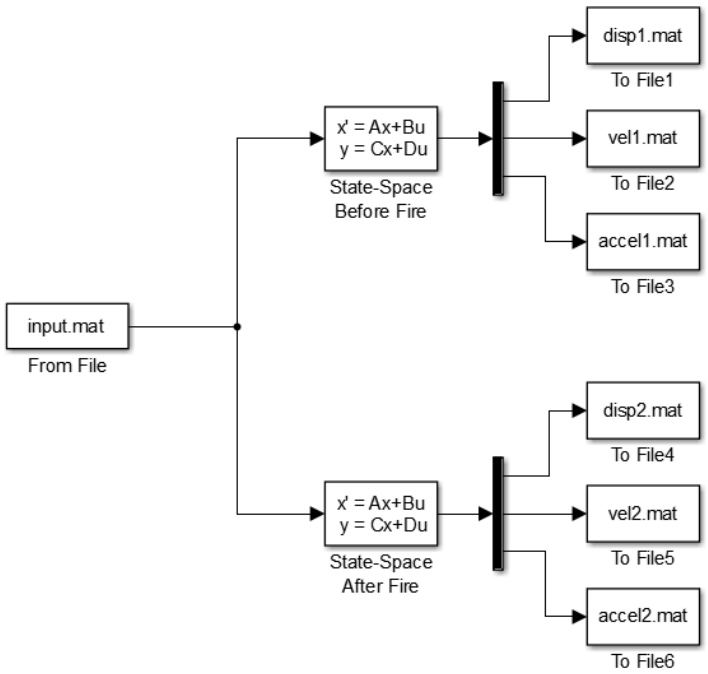

Figure 42 - Simulink Model

An important step in understanding dynamic behavior of a structure is to derive its natural frequency. Matlab was used to simplify the derivation of the natural frequency of the structure. The function “eig” returns variables for the eigenvalues and eigenvectors of a system defined by Equation 18. The following equations represent the derivation of natural frequency.

$$k * \varphi = m * \varphi * w_n \quad \textbf{Equation 23}$$

$$f_{ni} = \sqrt{w_{ni}}/(2 * \pi) \quad \textbf{Equation 24}$$

Where: k = stiffness matrix, m = mass matrix, w_{ni} = circular frequency, φ = modes, f_{ni} = natural frequency

Natural frequencies were calculated for the first five mode shapes as most structures tend to stay within this range of motion. It should be noted that the natural frequency represents the modal frequency of the entire structure. The following figure shows the graph of the natural frequencies of the first five modes for the theoretical structure.

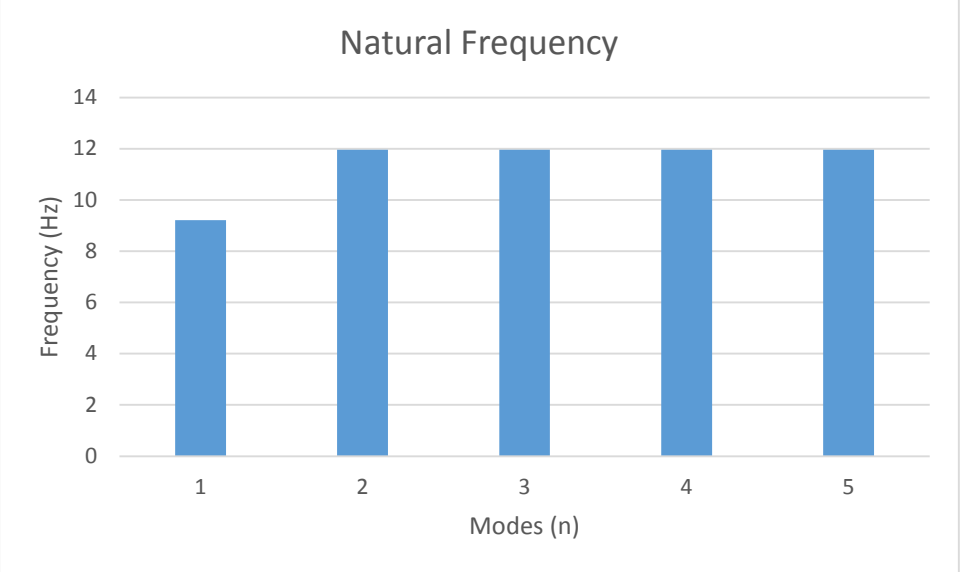

Figure 43 - Natural Frequency Graph

It is shown that the natural frequency varies between 9 and 12 Hz for the first 5 mode shapes of the structure. The only significant frequency shift occurs between the first and second modes. The following table provides a summary of the natural frequencies of the first 5 modes.

Table 5 - Natural Frequency Summary

Mode	Natural Frequency
1	9.215
2	11.962
3	11.963
4	11.964
5	11.964

Finally, the “Dynamic Analysis” code uses Fast Fourier Transform (FFT) to derive the dominant frequency of each element before and after the fire. The natural frequencies that were calculated using the “eig” function in Matlab represent the modal frequency of the entire structure, while the FFT function represents the frequency of an individual member. This means that the frequencies of the individual members may be slightly different than the natural modal frequency of the entire structure. An example and verification of Fast Fourier Transform can be found in Appendix F – Fast Fourier Transform Example.

The differences in acceleration and frequency are compared for a particular element, which changes based on the test. The three elements were chosen to represent three separated members within the structure. The dynamic results are reported in the subsequent sections of this chapter. The following figures depict the finite element model and nodes used for the dynamic model.

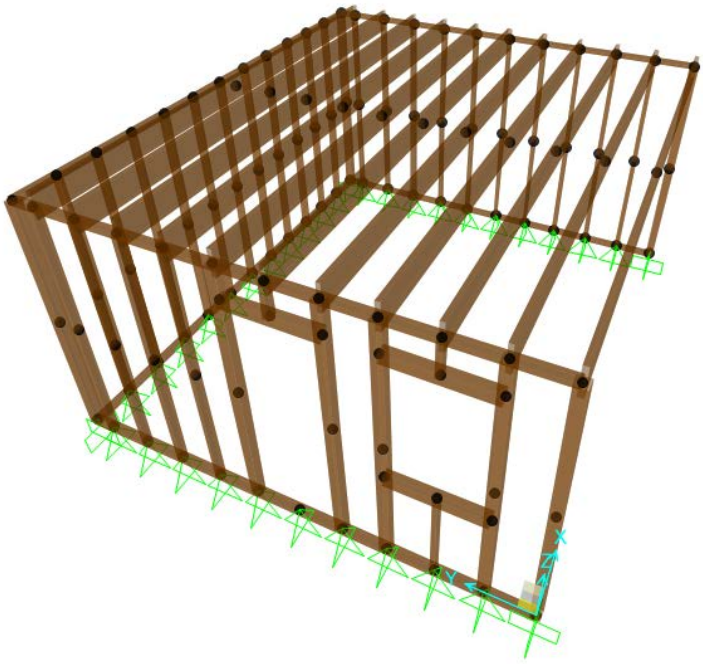

Figure 44 - Finite Element Model

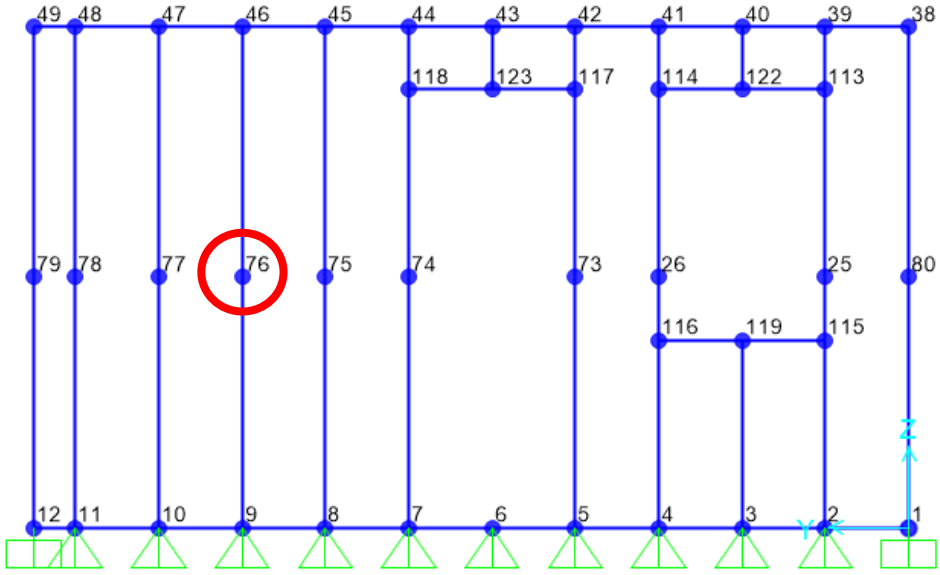

Figure 45 - Test 1 Node Point

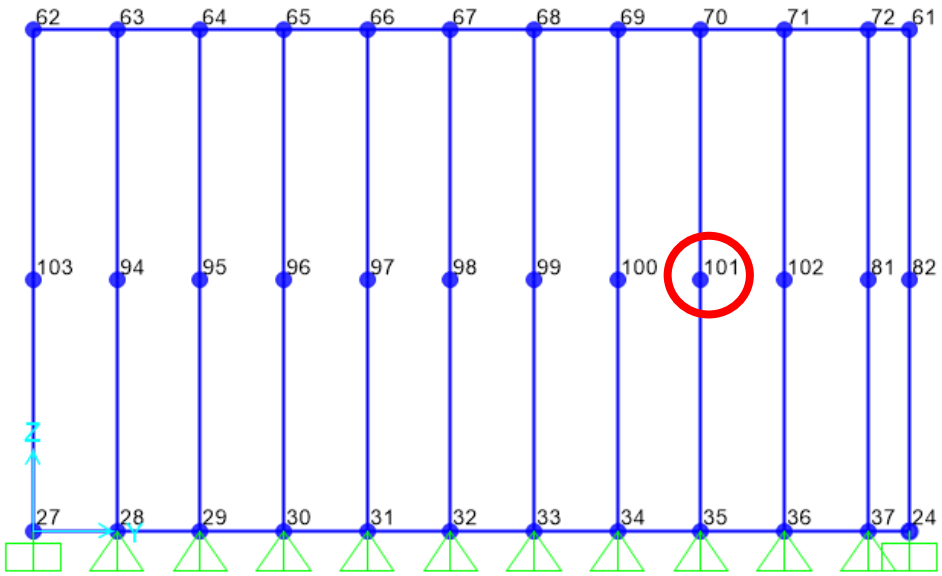

Figure 46 - Test 2 Node Point

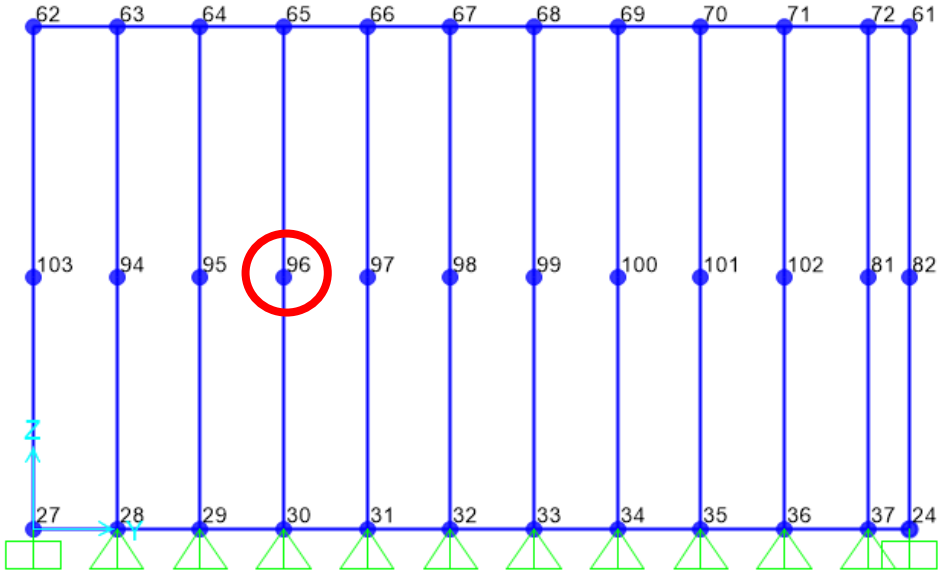

Figure 47 - Test 3 Node Point

The previous figures present the SAP2000 finite element model and the location of the nodes that were used for each of the three tests. Test 1 was performed on the wall with the door, and Tests 2 and 3 were performed on the wall opposite to the door. The equation numbers in Table 6

represent the axis of freedom that is assigned to each node to be used in Matlab. This number would match to a particular position within the mass and stiffness matrices. The following table represents the equations numbers that correspond with these nodes. The equation numbers refer to the location within the extracted matrices that correspond to the various degrees of freedom for each member.

Table 6 - Node Equation Numbers

Test Number	Node Number	Equation Number
1	76	20
2	101	2
3	96	49

3.2. Verification of Natural Frequency Calculations

The frequency calculated in Matlab was verified using the modal analysis feature in SAP2000. A column with a concentrated mass was modeled to check that its natural frequency matched using hand calculations, Matlab, and SAP2000.

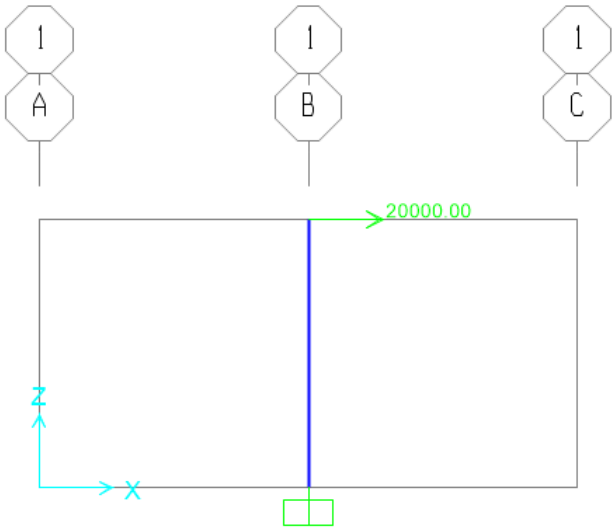

Figure 48 - Beam Verification Model

A 3 meter tall W18x40 column made of A992Fy50 steel was modeled in SAP2000. The base of the column was a fixed connection, and a twenty thousand kilogram mass was affixed to the top of the column. Metric units were used to avoid confusion in units that is sometimes present in the US/Imperial system. The following table contains the material properties that were used in the model.

Table 7 - SAP Verification Material Properties

M =	20000	kg
E =	2E+11	N/m^2
I =	0.000255	m^4
L =	3	m

The following equations represent the manual derivation of the mass and stiffness matrices. These values are used to check the frequencies calculated within the SAP2000 software. The mass is representative of a lumped mass placed at the center of the beam, and the stiffness is derived from an evenly distributed self-weight load that was used for the deflection of the beam.

$$M = 20000\ kg \quad \textbf{Equation 25}$$

$$K = \frac{3EI}{L^3} = \frac{3 * 2E11\ N/m^2 * 0.000255\ m^4}{(3\ m)^3} = 5.667E6\ N/m \quad \textbf{Equation 26}$$

$$f_n = \frac{1}{2\pi}\sqrt{\frac{K}{M}} = 2.679\ Hz \quad \textbf{Equation 27}$$

$$T = \frac{1}{f_n} = 0.373\ sec \quad \textbf{Equation 28}$$

Where: M = mass (kg), K = stiffness (N/m), f_n = natural frequency (Hz), T = period (s)

Table 8 - SAP2000 Example Modal Frequency Results

OutputCase	StepType	StepNum	Period	Frequency	CircFreq	Eigenvalue
Text	Text	Unitless	Sec	Cyc/sec	rad/sec	rad2/sec2
MODAL	Mode	1	0.385549	2.593705092	16.29672973	265.5833998

It was shown that the frequencies calculated through SAP2000 matched those derived through hand calculations fairly accurately. Differences in the values may come from the method that SAP2000 uses to calculate the stiffness of the structure. Finally, the “eig” function in Matlab yielded a natural frequency of 2.594 Hz, which matches the value derived in SAP2000.

After the natural frequency calculation was verified using the column example, SAP2000 was used to verify the natural frequencies calculated using the “eig” function in Matlab. The

following table represents the modal frequencies derived using SAP2000 for the full test structure.

Table 9 - SAP2000 Full Modal Frequency Results

OutputCase	StepType	StepNum	Period	Frequency	CircFreq	Eigenvalue
Text	Text	Unitless	Sec	Cyc/sec	rad/sec	rad2/sec2
MODAL	Mode	1	0.108518	9.215086943	57.90009888	3352.421451
MODAL	Mode	2	0.083597	11.96219236	75.1606713	5649.12651
MODAL	Mode	3	0.083589	11.96335986	75.16800689	5650.22926
MODAL	Mode	4	0.083585	11.96380097	75.1707785	5650.64594
MODAL	Mode	5	0.083585	11.96392439	75.17155394	5650.762521
MODAL	Mode	6	0.083584	11.96399345	75.17198784	5650.827755
MODAL	Mode	7	0.083584	11.96402628	75.17219415	5650.858773
MODAL	Mode	8	0.083584	11.96404735	75.17232651	5650.878673
MODAL	Mode	9	0.083584	11.9640593	75.17240163	5650.889966
MODAL	Mode	10	0.083584	11.96406683	75.17244891	5650.897076
MODAL	Mode	11	0.083584	11.96407074	75.17247348	5650.900769
MODAL	Mode	12	0.082633	12.10169994	76.03722323	5781.659316

These values exactly match the natural frequencies calculated using the “eig” function in Matlab as shown in Table 5. This verifies that the natural modal frequencies derived in Matlab are accurate according to SAP2000.

The example column was then tested using the FFT function in Matlab to derive the acceleration and frequency response. The impact force from “Test 1” was used to check the response of the example column. That data was used purely as a theoretical force. The specifics on Modal Test 1 can be found later in this report. The following figures represent the dynamic response of the example column as derived by Matlab.

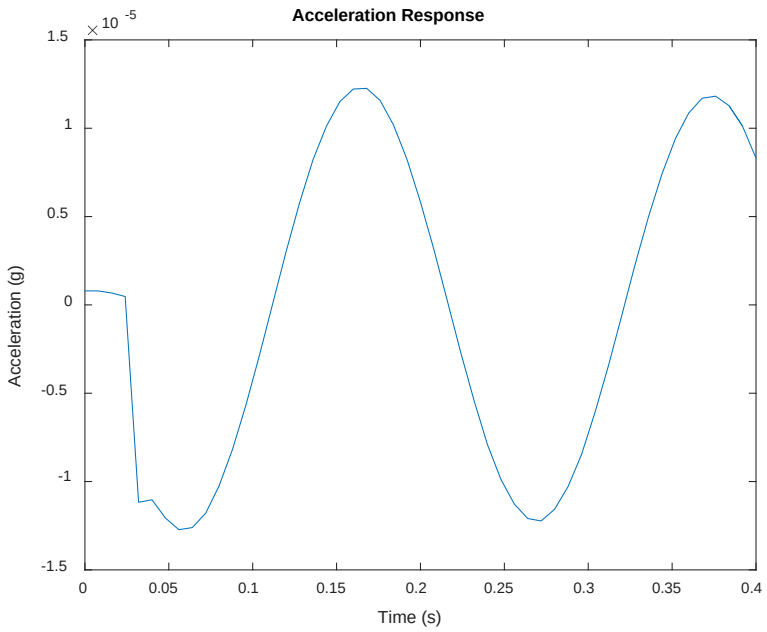

Figure 49 - Example Column Acceleration Response

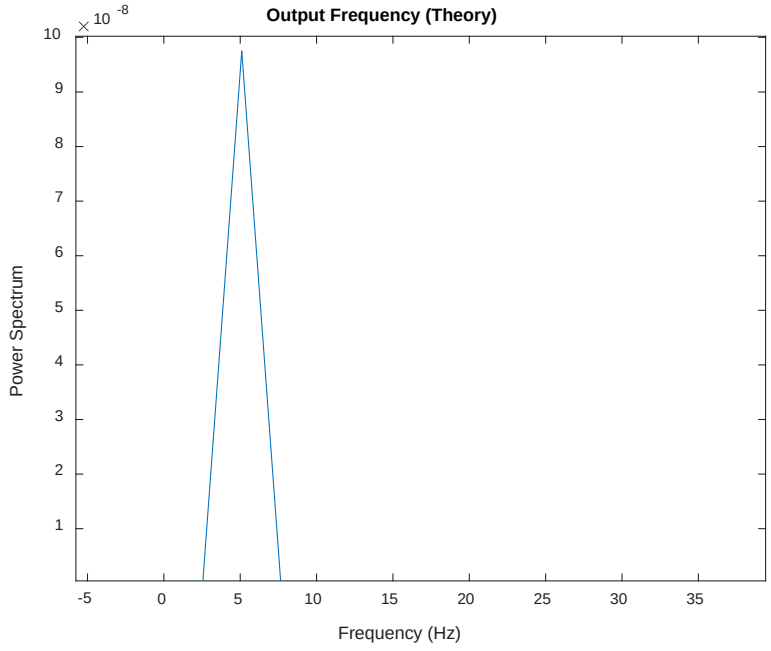

Figure 50 - Example Column Frequency Response

The maximum acceleration response was 1.272e-05 g and the dominant output frequency was 5.101 Hz. Comparatively, the natural modal frequency calculated through hand calculations and SAP2000 yielded a value of 2.679 Hz. This shows that the frequency response of the individual member does not necessarily match the natural modal frequency of the entire structure. This known example is verification of the SAP2000 model frequency results.

3.3. Modal Hammer Input Data

An initial test was performed with a modal hammer in order to obtain a theoretical input force that could be used with the dynamic model. The hammer measures the input force with an internal accelerometer built into the hammer. Three different tests were performed with the hammer alone to acquire three different sets of input force data that could be used with the dynamic model. For these tests, a relatively small impact force was applied over a very small duration of time to simulate an actual modal test.

Figure 51 **- Modal Hammer**

The following graph represents the time history of the impact force applied with the modal hammer. The actual time period of the impact was extremely brief, so the data collection time interval had to be very small. Some data points would be lost if the collection time interval were too large and that would result in an inaccurate frequency. The input force time history was used to derive the input frequency spectrum.

Test 1

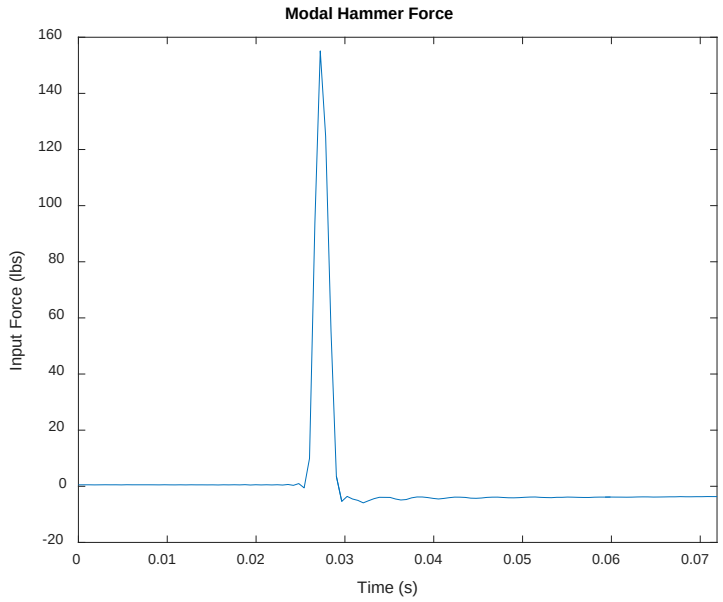

Figure 52 - Modal Hammer Force (Test 1)

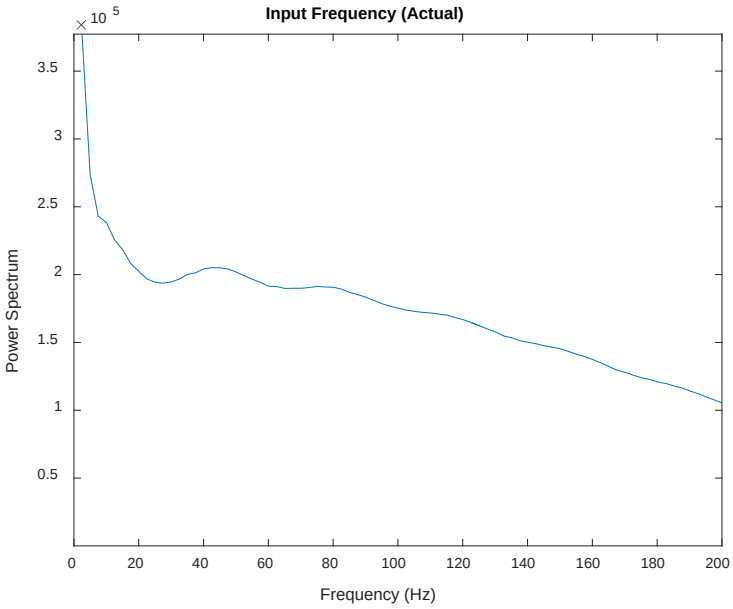

Figure 53 - Input Frequency Spectrum (Test 1)

Test 2

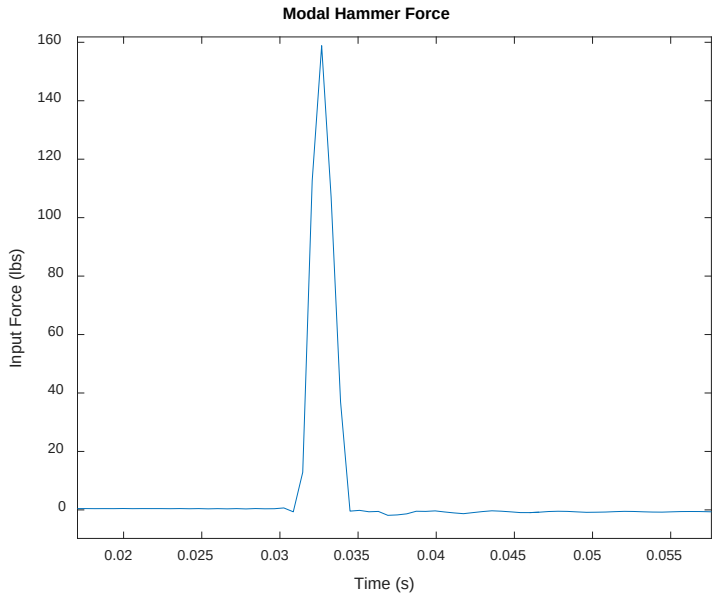

Figure 54 - Modal Hammer Force (Test 2)

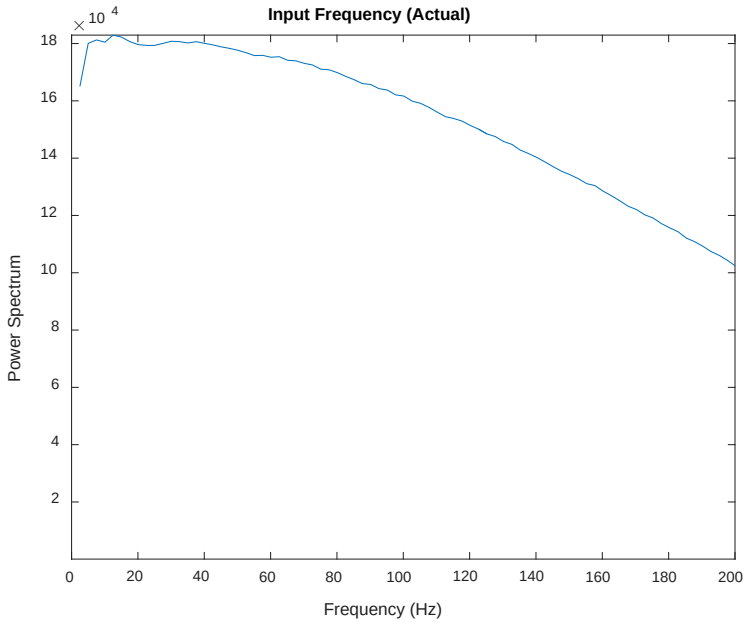

Figure 55 - Input Frequency Spectrum (Test 2)

Test 3

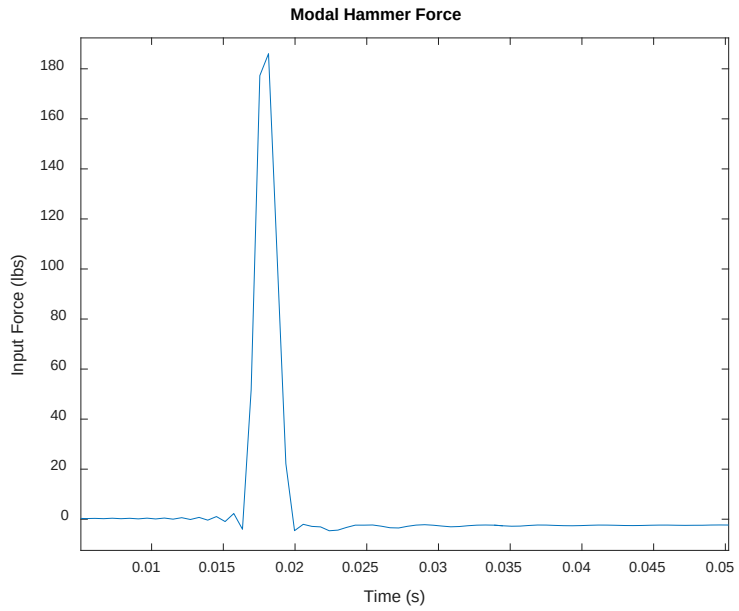

Figure 56 - Modal Hammer Force (Test 3)

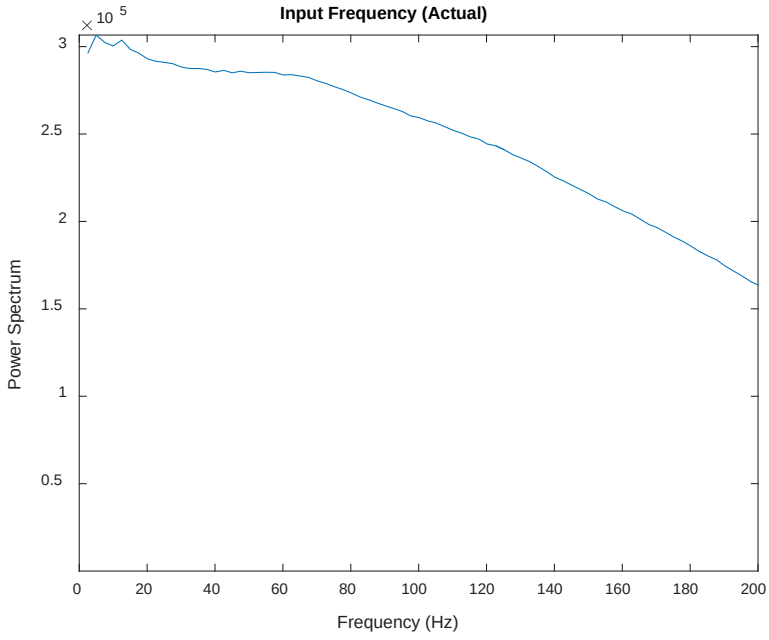

Figure 57 - Input Frequency Spectrum (Test 3)

The previous graphs represent the input force and frequency exerted by the modal hammer. The frequency was derived through the use of the Fast Fourier Transform within Matlab. Multiple frequencies are present within the input force frequency spectrum, which is expected from impulse loads during modal testing according to a resource called *The Fundamentals of Modal Testing* **[25]**. Modal hammers are meant to excite all modes of a structure which may correspond to this behavior. The following figures are from *The Fundamentals of Modal Testing.*

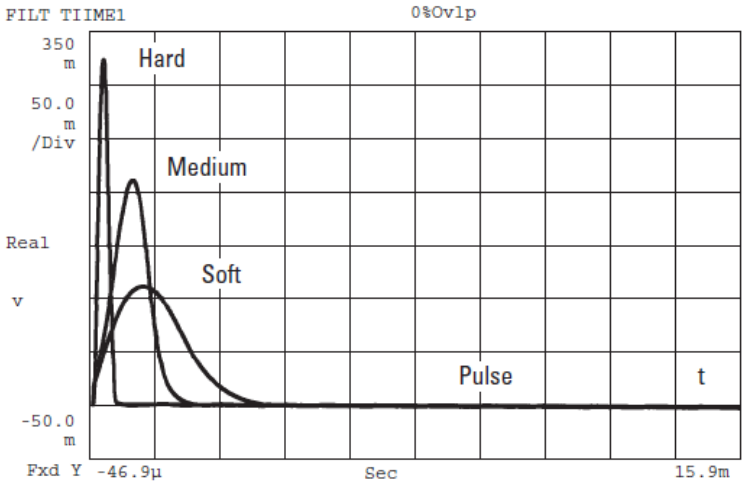

Figure 58 - Modal Hammer Hardness Levels

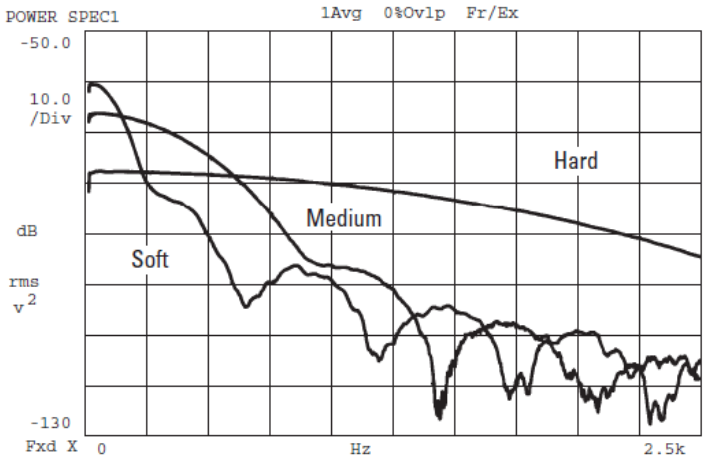

Figure 59 - Typical Modal Hammer Frequency Spectrum

The primary purpose of this test was to provide an input force data set to be used with the theoretical dynamic model. This would theoretically simulate an actual modal test. The following table summarizes the input data collected during the three modal tests.

Table 10 - Impact Force

Test Number	Node Number	Impact Force (lbs)
Test 1	76	150
Test 2	101	160
Test 4	96	180

The forces were kept in the same relative magnitude for all three tests. Theoretically, a larger impact force would provide a larger dynamic response. The frequencies were calculated based on the frequency spectrum created by the Fast Fourier Transform in Matlab, which is detailed later in this report.

3.4. Theoretical Ambient Dynamic Model

This section details the dynamic response of the theoretical light, wood-framed structure before a fire. Both Matlab and Excel were used in combination to create this model. The input force time history data collected from the impact hammer was used to test the model and yield an acceleration response for the given force. The state-space equation was used to calculate displacement, velocity, and acceleration data for the theoretical model. Fast Fourier Transform was used to derive the frequency from the acceleration response. Acceleration and frequency were the main focus of this project, as accelerometers are a very common method of measurement in the industry. It should be noted that the ambient model cannot be validated at this time, but it may be tested in the future by the DHS Green Building Project team.

The following figures in this section represent the dynamic response in regard to acceleration and frequency of the theoretical structure during ambient conditions. The tests were performed on the three separate locations that were detailed earlier in this report. Summary tables are provided at the end of this section to detail the quantitative values of acceleration and frequency for each test location. The acceleration figures show a magnified view of the dynamic response of the theoretical model. The acceleration is measured in “g” (32.2 ft/s) and the time is measured in seconds. The output frequency figures show the frequency spectrum in Hz (hertz) for the theoretical model. The maximum value with the power spectrum for each frequency graph corresponds to the dominant frequency of the dynamic response.

Test 1

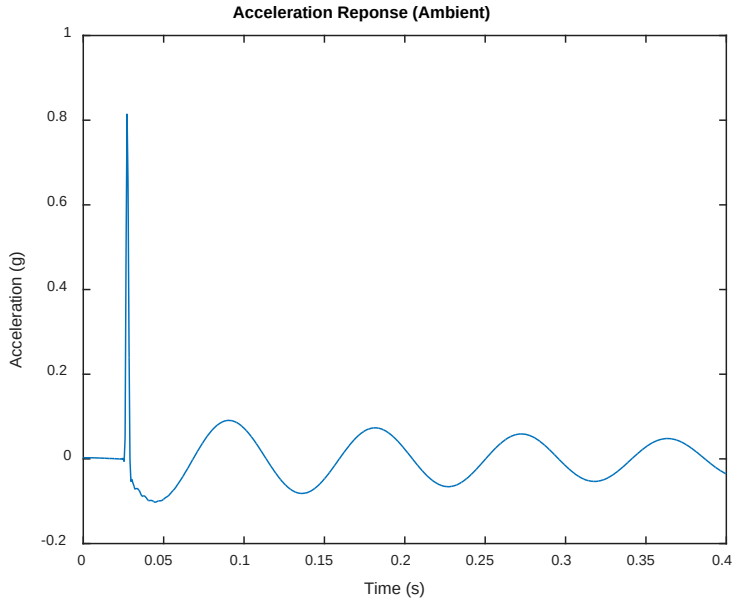

Figure 60 - Ambient Acceleration (Test 1)

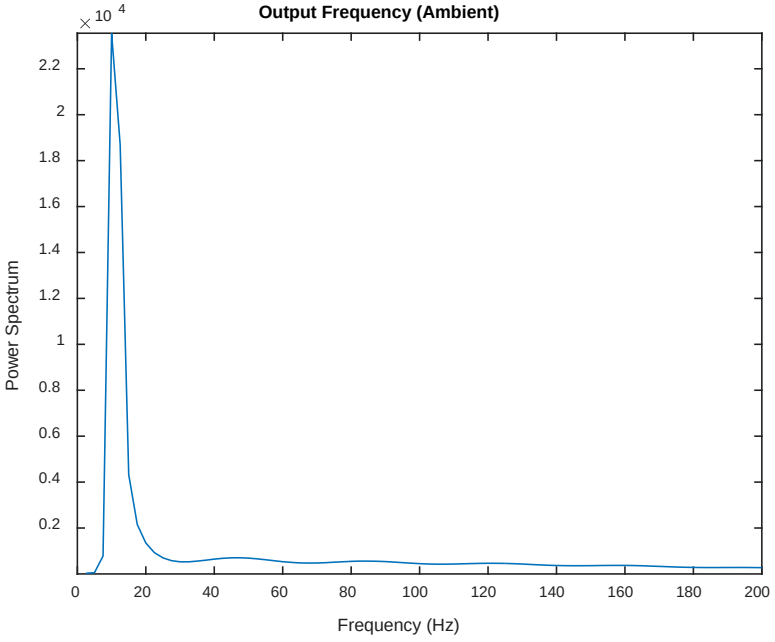

Figure 61 - **Ambient** Output Frequency (Test 1)

Test 2

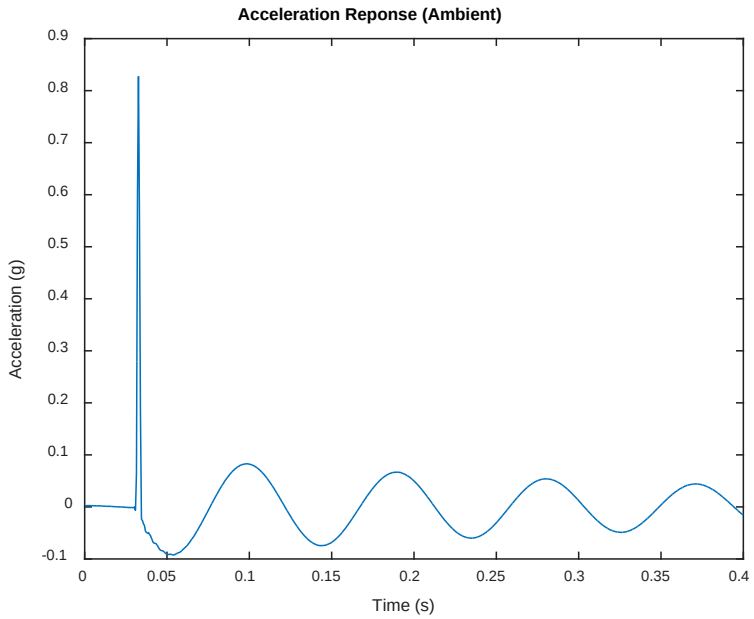

Figure 62 - Ambient Acceleration (Test 2)

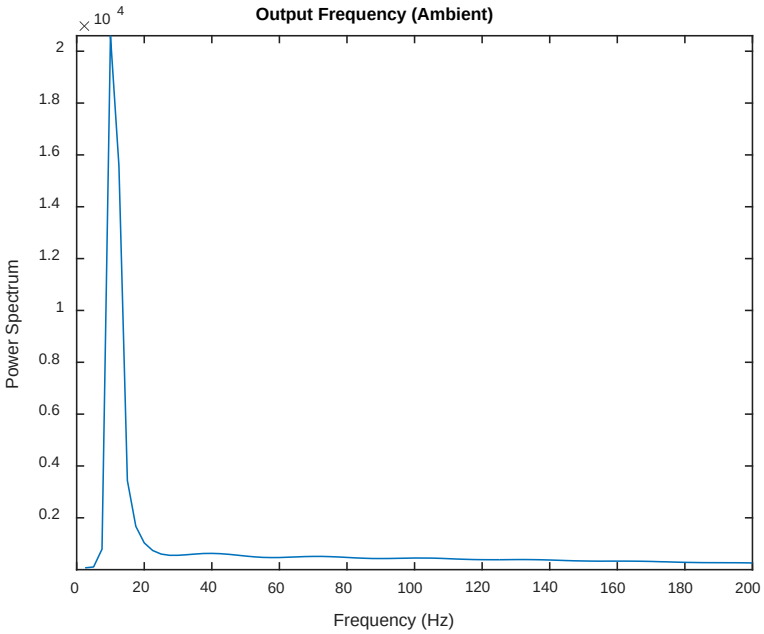

Figure 63 - Ambient Output Frequency (Test 2)

Test 3

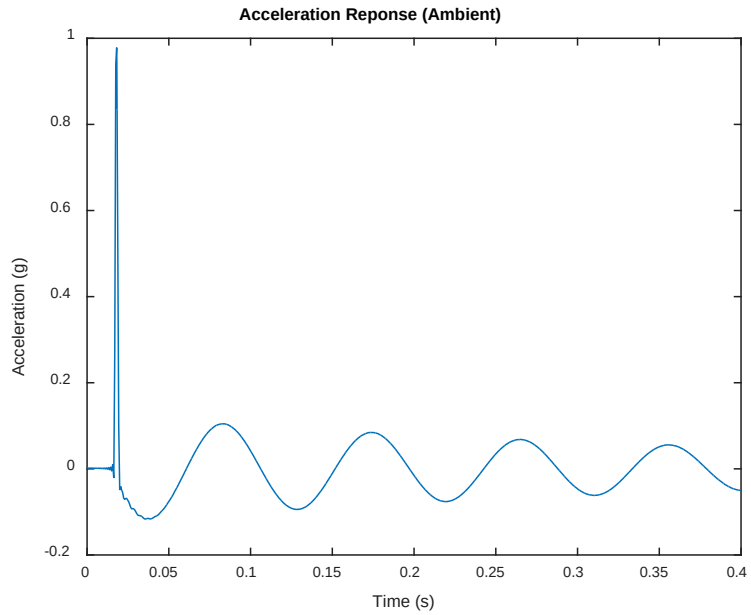

Figure 64 - Ambient Acceleration (Test 3)

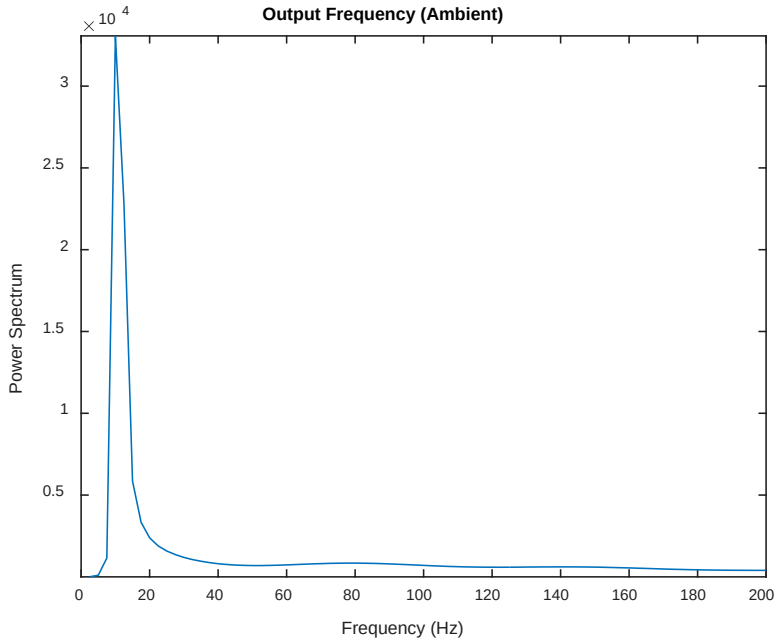

Figure 65 - Ambient Output Frequency (Test 3)

The following table summarizes the dynamic response of the theoretical structure.

Table 11 - Ambient Dynamic Response Comparison Summary

Test Number	Acceleration (g)	Frequency (Hz)
1	0.815	10.004
2	0.827	10.004
3	0.978	10.004

Possible error within the dynamic model may have come from the assumptions made in the structural analysis model used to export the matrices. Simplifications were made in the model such as ideal pinned connections, uniform material properties, and lack of supplementary elements. Actual light, wood-framed structures contain semi-rigid connections that are somewhere between a pinned and fixed connection. Wood is not a uniform material as the members contain defects that alter the structural properties. Actual Structures are also built with blocking between the studs and joists, which significantly increases the stiffness of the overall system.

It was observed that the dominant output frequencies did fall within the range of the natural frequencies for the first five modes. The natural frequency for the test structure ranged from 9 to 12 Hz, while the output frequency measured by the dynamic model was close to 10 Hz. The "eig" function was used to calculate the natural modal frequency of the entire structure, while FFT was used to calculate the frequency of an individual member.

It should be noted that all work in the ambient dynamic model is theoretical and cannot be validated through testing at this time. The structure was chosen in anticipation of possible testing by the DHS Green Building Project team in the future. They plan for testing that may be able to validate both the static model for their project and the dynamic model for this project. This work presents the framework for a theoretical dynamic response prediction model.

3.5. Theoretical Results after a Fire

The purpose of this section is to provide a summary of the predicted dynamic response after a fire using the dynamic model. The dynamic model was modified to predict the acceleration response of the structure after the simulated fire. The model was tested using the input force from the modal hammer. Conclusions are made based on the varying behavior of acceleration and frequency shifts after a fire.

It should be noted that the dynamic response of the structure after the fire cannot be validated through testing at this time. Validation was not possible through testing for the dynamic model before and after a fire, so it was excluded from this scope of this project. This is a possible area of study for the DHS Green Building Project team when they begin testing in the WPI Gateway Fire Lab. The DHS Green Building Project plans to carry out testing in the WPI Gateway Fire Lab in the near future, in which they may be able to validate both the static and dynamic theoretical models. This project provides a theoretical prediction model for the baseline of future research.

The main reason for the differences in acceleration and frequency after the fire is the change in matrices used for the dynamic analysis. This change is due to the reduction of the mass and stiffness matrices due to thermal degradation. The following graphs represent the theoretical dynamic response comparison before and after a fire.

Test 1

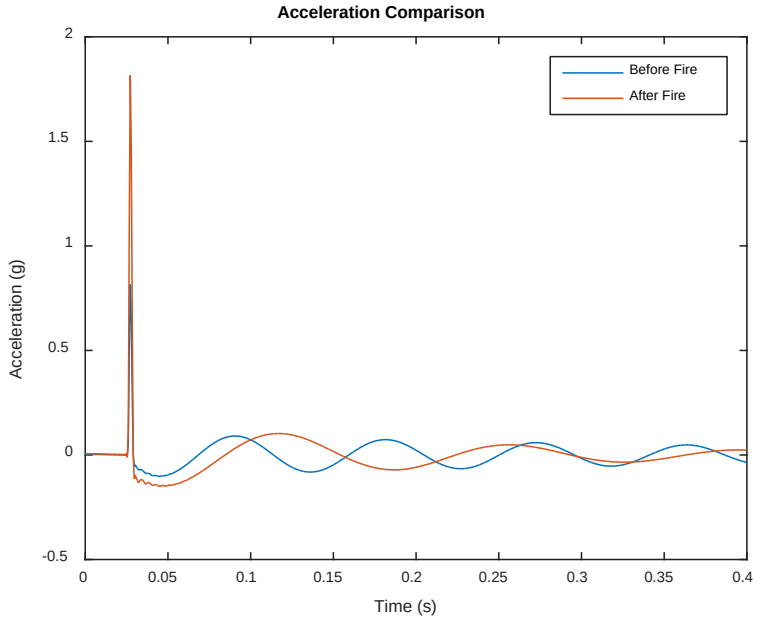

Figure 66 - Acceleration Comparison (Test 1)

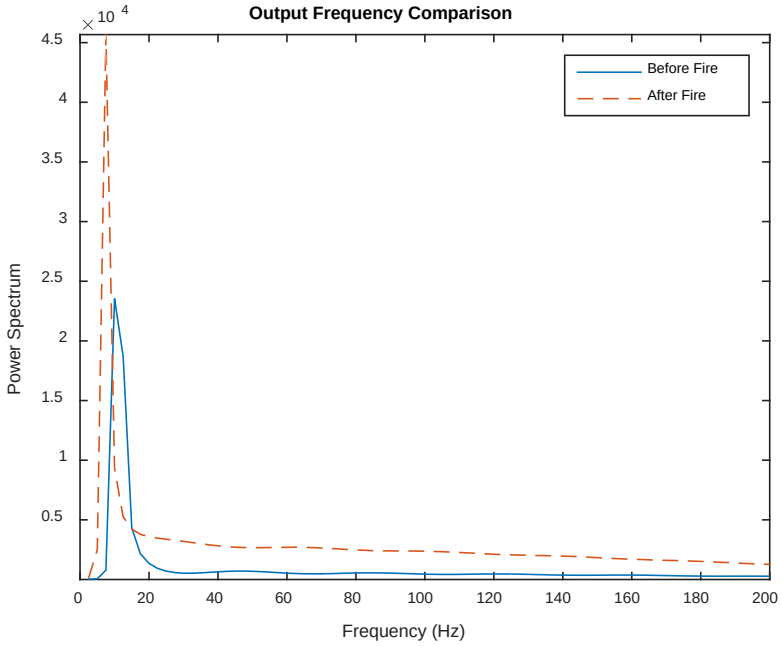

Figure 67 - Output Frequency Comparison (Test 1)

Test 2

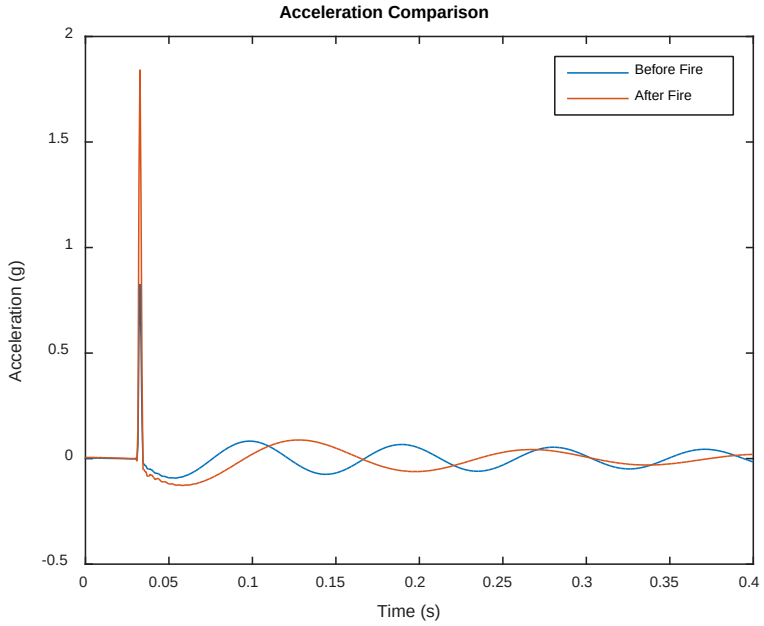

Figure 68 - Acceleration Comparison (Test 2)

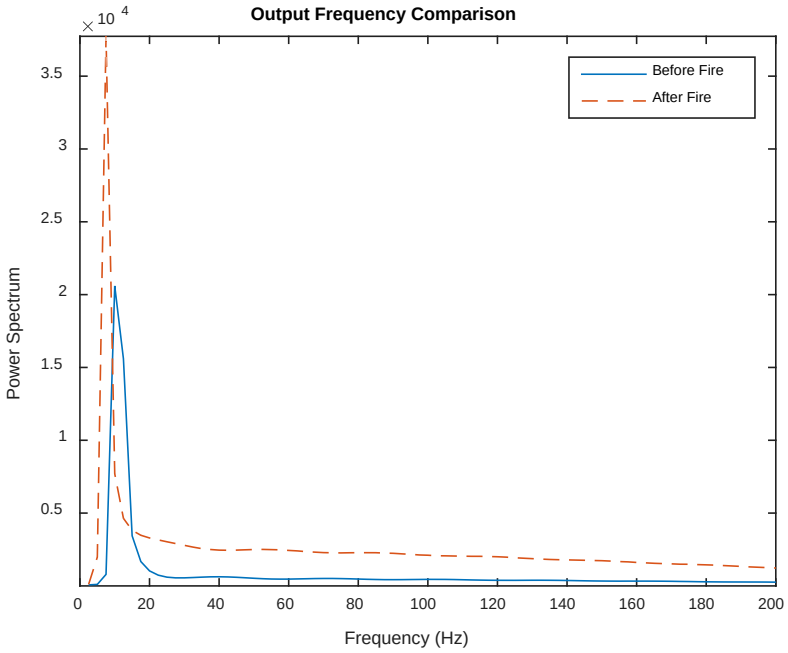

Figure 69 - Output Frequency Comparison (Test 2)

Test 3

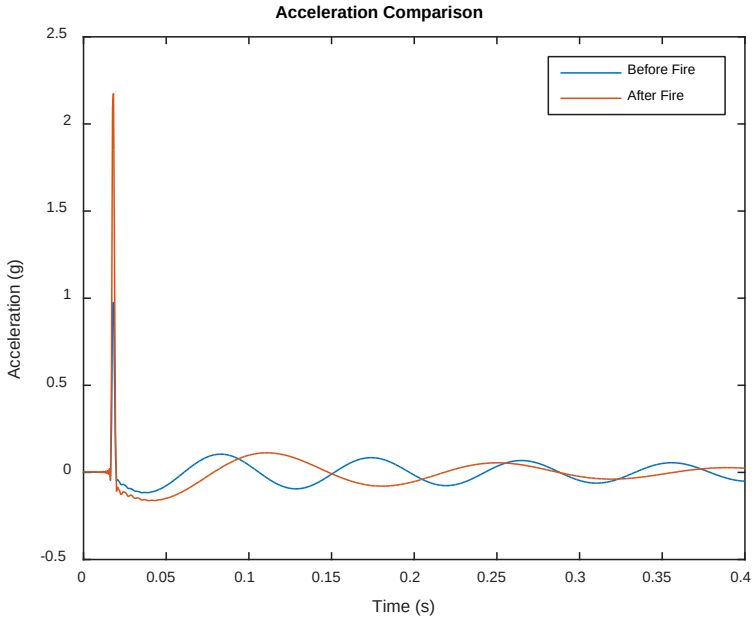

Figure 70 - Acceleration Comparison (Test 3)

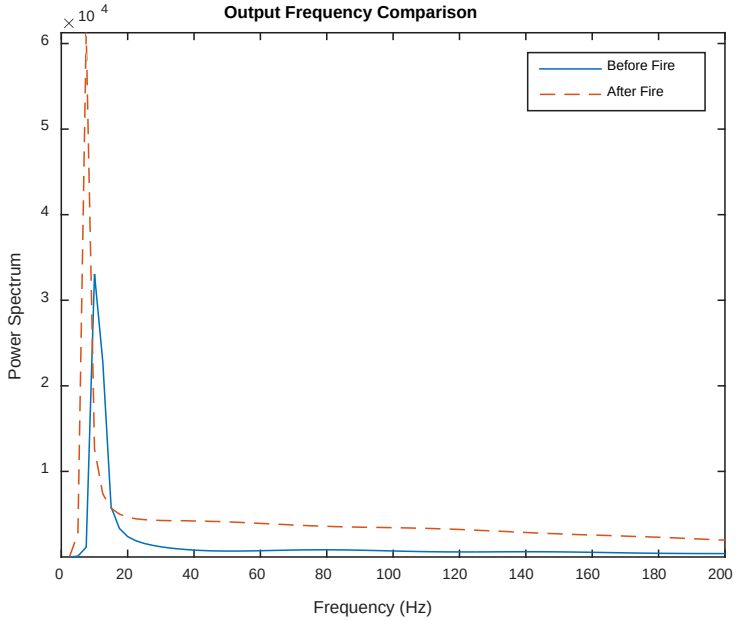

Figure 71 - Output Frequency Comparison (Test 3)

The maximum power in the frequency graphs corresponds to the dominant frequency chosen for the member. The following table summarizes the results obtained from Matlab for the dynamic model. These results represent the general behavior that is expected to result before and after the fire.

Table 12 - Theoretical Acceleration Summary

Test Number	Acceleration (g) Before Fire	Acceleration (g) After Fire	Percent Change
1	0.815	1.816	122.8%
2	0.827	1.843	122.9%
3	0.978	2.175	122.4%

Table 13 - Theoretical Frequency Summary

Test Number	Frequency (Hz) Before Fire	Frequency (Hz) After Fire	Percent Change
1	10.004	7.503	25.0%
2	10.004	7.503	25.0%
3	10.004	7.503	25.0%

It is shown that the acceleration response increases over 120% after a fire for all three tests. The output frequency decreases by approximately 25% after a fire for each test as well. There was a significant change for both the acceleration and the frequency. Each test had similar frequency shifts as the same thermal degradation was applied to every element in the theoretical model. Actual fires have concentrations of temperature and heat flux at various locations. These shifts in acceleration and frequency are the primary trends to be observed in this project.

3.6. Results Summary

This section provides a general summary of the results obtained from the dynamic analysis. The theoretical dynamic response of the structure was compared before and after a fire. The shifts in dynamic response are the key concept to learn from this project.

The theoretical model calculated the dynamic response of the structure before and after a fire. The following figures summarize the comparison between the theoretical dynamic responses of the structure in both scenarios.

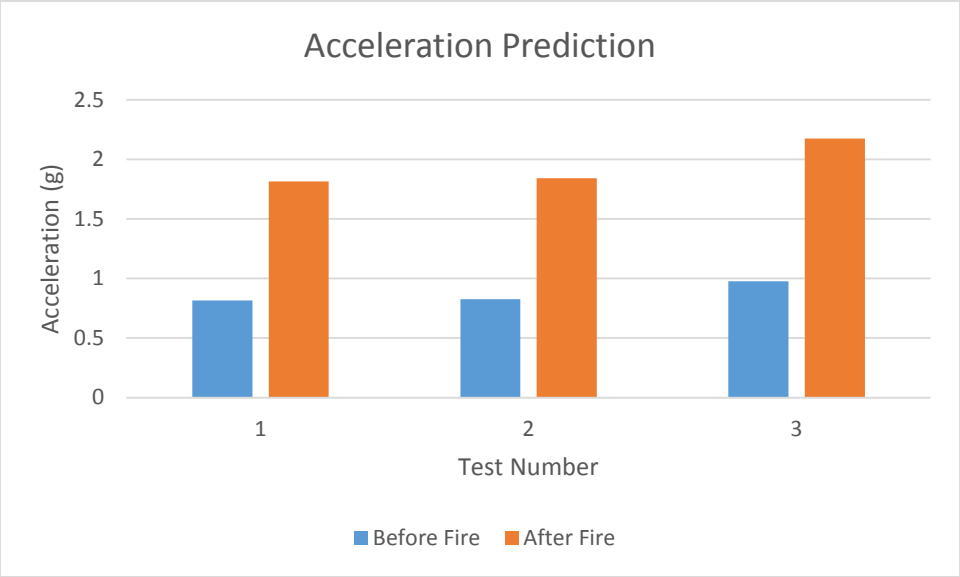

Figure 72 - Acceleration Prediction Graph

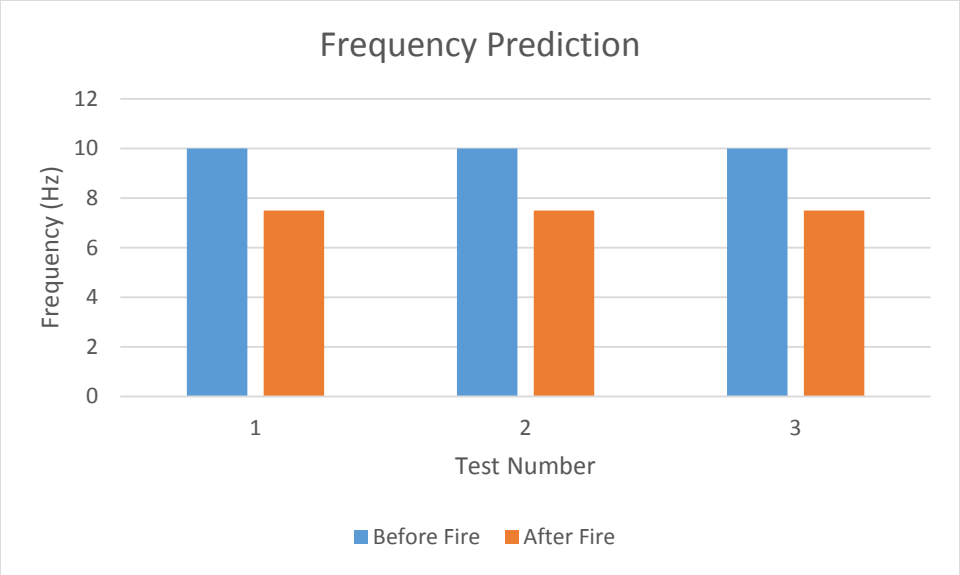

Figure 73 - Frequency Prediction Graph

The results of prediction study show that the acceleration response increases by over 120% and the output dominant frequency decreases by 25% after a fire. Note that the magnitudes of the acceleration and frequency response represent the test structure that was chosen through the condensed study of the DHS Green Building Project in anticipation of future testing. The magnitudes may not represent those of a full-sized structure. However, the shifts in acceleration and frequency may translate to larger structures, which is helpful in understanding the effect of fire upon dynamic response.

The dynamic models for before and after a fire could not be validated for this project. The DHS Green Building Project team may be able to validate the dynamic model before and after a fire in the near future by conducting tests in the Gateway Fire Lab. The theoretical dynamic response data presented by this project can be used as a baseline for lab testing in future projects.

4. Conclusions

4.1. Project Conclusion

Structural dynamic analysis is used to learn about the response of buildings in motion, but it can also be used to assess the integrity of the structure. Structural health monitoring has been used to predict damage within buildings after earthquakes and other major events. This same concept can be applied to wood structures during fire conditions. A structure becomes damaged by fire in the same manner as it would be damaged by an earthquake or explosion. This project provided a starting point for the dynamic analysis of light, wood-framed structures during fire conditions.

This project presented a theoretical method to model a simple structure after a fire event by making appropriate assumptions. The geometry of the wood members was degraded due to the charring effect of wood exposed to fire, which affected the mass and stiffness of the system. As the dynamic response of a structure depends on the mass and stiffness matrices, the theoretical dynamic response shifted after a simulated fire event. A typical fire was modeled using FDS to obtain heat flux values that were used to degrade the structural members. The heat flux data from FDS was analyzed in Excel and then extracted to Matlab. Matlab was the primary tool for the creation of the dynamic analysis tool.

The theoretical model was created to predict the dynamic response of the light, wood-framed structure before and after a fire. The acceleration and frequency data was derived using Matlab. A source of the error within the calculations may have been the simplified assumptions made when creating the structural analysis model used to export the matrices. The shift in acceleration

and frequency is an important factor for the theoretical model after the fire. The dynamic model and structural reduction method created for this project can serve as a baseline for similar projects. Although the small, condensed structure that was used for this project may not represent the exact magnitude of acceleration and frequency of a full-sized structure, the shifts in these values are the key aspect investigated by this project.

Validation of the theoretical dynamic model for before and after a fire was not possible through testing at this time. This project was a collaborative effort with the DHS Green Building Project in anticipation of potential future testing which could be used to validate both the static model used for their project and the dynamic model used for this thesis. This project presents a theoretical method of structural thermal degradation to predict the dynamic response of a structure after a fire.

The degradation in mass and stiffness matrices for light, wood-framed structures may be predicted by analyzing the degradation in cross sectional area due to charring. Frequency shifts could occur in wood structures during a fire as predicted by this research, which would indicate structural damage. Structural health monitoring methods could be applied in the same manner as it is used currently in industrial applications. The dynamic model is the first step in predicting this structural damage.

4.2. Recommendations for Future Work

There were several topics that were not included in the scope of investigation for this project. The first area of interested would be the investigation of degrading elastic modulus and how it affects the dynamic response of the system. Past research has developed a temperature correlation of elastic modulus for various types of wood material at low temperatures. Studies should be performed to find higher temperature correlations for temperatures past flashover conditions. This correlation would allow a more accurate dynamic model to be created.

Another future area of research would be the effects of changing wood density of the dynamic response of a structure. This project assumed the mass was lost in a direct relationship with the degrading cross sectional area. A more accurate method would be to find the temperature correlation of density and use that data to adjust the mass of the members as the sections degrade. This would lead to a further reduced mass matrix and would change the dynamic response of the system.

A third future are of investigation is the effect of temperature on the damping of a structural system. This project focused on the dynamic effect of degrading the mass and stiffness matrices. The damping matrix was creating using the Rayleigh method. In reality, the damping coefficients used in the Rayleigh method would most likely change with elevated temperatures. The damping matrix plays a large role in the dynamic response of a structure, and its degradation would likely lead to a significant shift in the frequency of the system.

The fundamentals presented in the project could ultimately be used to create a dynamic failure model for light, wood-framed structures during fires. Frequency shifts that are used in industrial applications could be used to indicate critical damage within a structure. Potentially, a mobile unit could be used that would send a known dynamic pulse throughout a building and would be able to receive vital information by analyzing the frequency response. This could be installed in buildings with Fire Control Systems to be used by both firefighters and other emergency professionals during a fire. Buildings equipped with accelerometers (high-rise buildings) could pinpoint precise structural damage before, during, and after fires. This would ease the inspection process and make precision repair more feasible. This knowledge could produce a better understanding of the overall fire performance of buildings and the time to collapse, preventing loss in human life.

Appendix

Appendix A – Fast Fourier Transform Example

The following example shows the execution of the Fast Fourier Transform upon the known equation of y = sin(x). Matlab was used to implement the FFT calculation.

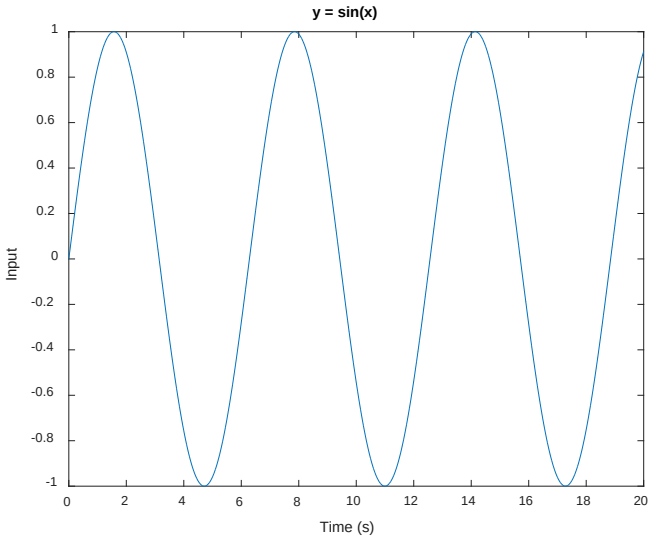

Figure 74 - FFT Example Time History

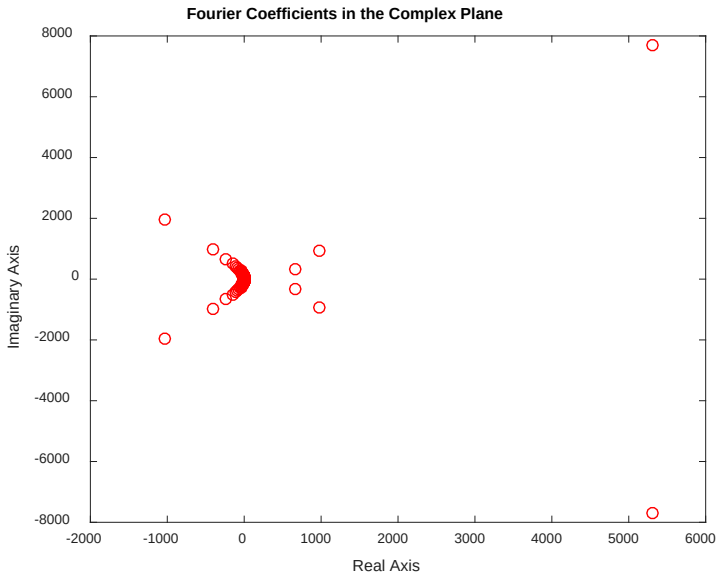

Figure 75 - FFT Example Fourier Coefficients

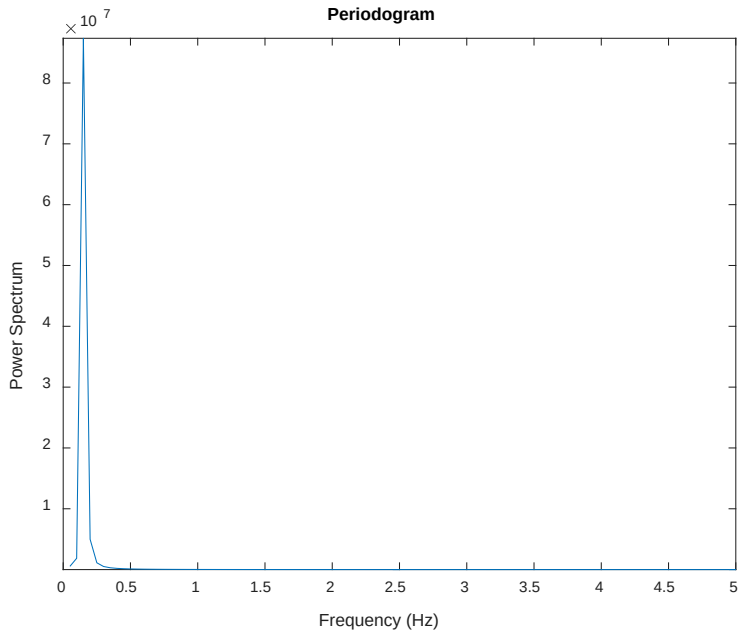

Figure 76 - FFT Example Periodogram

The FFT analysis yielded a dominant frequency of 0.15 Hz and a period of 6.67 seconds. This means that 1 cycle of the time history graph would be completed in 6.67 seconds. This period can be seen clearly on the time history graph, which confirms the accuracy of the FFT calculation.

Appendix B – Span Tables

SOUTHERN PINE SPAN TABLES

Maximum spans given in feet and inches inside to inside of bearings

TABLE 5 FLOOR JOISTS – 40 PSF LIVE LOAD, 20 PSF DEAD LOAD, 360 DEFLECTION

Size (inches)	Spacing (inches on center)	Grade									
		Visually Graded				Machine Stress Rated (MSR)			Machine Evaluated Lumber (MEL)		
		DSS	No.1	No.2	No.3	2400f - 2.0E	1650f - 1.5E	1500f - 1.6E	M-14 (1800-1.7)	M-29 (1550-1.7)	M-12 (1600-1.6)
2x6	12.0	11-4	10-9	9-10	7-5	11-7	10-6	10-9	10-11	10-11	10-9
	16.0	10-4	9-9	8-6	6-5	10-6	9-6	9-9	9-11	9-11	9-9
	19.2	9-8	9-0	7-9	5-11	9-10	9-0	9-2	9-4	9-4	9-2
	24.0	9-0	8-1	6-11	5-3	9-2	8-4	8-6	8-8	8-8	8-6
2x8	12.0	15-0	14-2	12-6	9-5	15-3	13-10	14-2	14-5	14-5	14-2
	16.0	13-7	12-7	10-10	8-2	13-10	12-7	12-10	13-1	13-1	12-10
	19.2	12-10	11-5	9-10	7-5	13-0	11-10	12-1	12-4	12-4	12-1
	24.0	11-11	10-3	8-10	6-8	12-1	11-0	11-3	11-5	11-5	11-3
2x10	12.0	19-1	16-11	14-9	11-5	19-5	17-8	18-0	18-5	18-5	18-0
	16.0	17-4	14-8	12-10	9-10	17-8	16-0	16-5	16-9	16-9	16-5
	19.2	16-4	13-5	11-8	9-0	16-7	15-1	15-5	15-9	15-9	15-5
	24.0	15-2	12-0	10-5	8-1	15-5	14-0	14-4	14-7	14-7	14-4
2x12	12.0	23-3	20-1	17-5	13-6	23-7	21-6	21-11	22-5	22-5	21-11
	16.0	21-1	17-5	15-1	11-8	21-6	19-6	19-11	20-4	20-4	19-11
	19.2	19-10	15-11	13-9	10-8	20-2	18-4	18-9	19-2	19-2	18-9
	24.0	18-5	14-3	12-4	9-6	18-9	17-0	17-5	17-9	17-8	17-5

Maximum spans: southern pine joists & rafters

Appendix C – Char Rates

The following table was taken from the *Fire Safety Journal* article by Babrauskas. It details the char rate of various configurations of floor panels from multiple studies.

Table 14 - Char Rate Tests on Floors and Panels

Author	Specimen	Edges	Test	Load	Flame-through (min)	Effective charring rate (mm/min)
McNaughton	19 mm soft-, hardwoods	none†	small-scale	N	22 – 28	0.68 – 0.86
Holmes	12.7 mm flakeboard	none†	small-scale	N	11.5 – 16	0.79 – 1.10
White	24 – 32 mm panels	none†	small-scale	N	25 – 43	0.72 – 0.96
White et al.	18.2 mm plywood	T&G	E 119	Y	12 – 15	1.2 – 1.5
Son	12.7 mm plywood	blocking	E 119	Y	11.0	1.16
Son	12.7 mm plywood	blocking	small-scale	Y	9.42	1.35
Son	15.9 mm plywood	T&G	E 119	Y	11.83	1.34
Son	15.9 mm plywood	T&G	small-scale	Y	11.58	1.37
Son	2×12.7 mm plywood	plain	E 119	Y	13.5	1.88
Son	2×12.7 mm plywood	plain	small-scale	N	21.7	1.17
Son	2×12.7 mm plywood	plain	small-scale	Y	17.3	1.47
Son	19.8 mm pine	T&G	small-scale	Y	10.5	1.89
Son	20.6 mm oak	T&G	small-scale	Y	14.17	1.45
Fang	18.3 mm plywood	T&G	E 119	Y	16.1–17.6	1.04 – 1.14
Fang	18.3 mm plywood	T&G	higher temp.	Y	6.1 – 9.2	2.0 – 3.0
Fang	15.9 mm plywood	T&G	room	Y	10.28	1.55
Fang	18.3 mm plywood	T&G	room	Y	12.03	1.52
Shoub	19 mm plywood	T&G	E 119	Y	3.5	5.4
Price	19 mm plywood	T&G*	E 119	Y	7.5	2.5
Price	18.3 mm plywood +PVC	T&G*	E 119	Y	7.4	2.5
Schaffer	19 mm plywood	unknown	E 119	Y	7.5	2.53
Richardson	38 mm boards, 0 mm gap	plain	E 119	N	24.3	1.56
Richardson	38 mm boards, 1 mm gap	plain	E 119	N	13.2	2.9
Richardson	38 mm boards, 2 mm gap	plain	E 119	N	4.5	8.4
Richardson	38 mm boards, 0 mm gap	T&G	E 119	N	33.6	1.13
Richardson	38 mm boards, 2.5 mm gap	T&G	E 119	N	18.1	2.1
Richardson	38 mm boards, 4 mm gap	T&G	E 119	N	17.8	2.1
White	55 mm boards, 2 mm gap	T&G	small-scale	N	44.4	1.2
White	55 mm boards, 0 mm gap	plain	small-scale	N	64	0.86
Haller	110 mm boards, nailed	plain	ISO 834	N	23.0	4.8
Bryan	12.7 mm softwoods	none†	jet fire	N	3.1 – 4.4	2.9 – 4.1
Bryan	12.7 mm oak	none†	jet fire	N	8.2	1.55
Bryan	12.7 mm softwoods	none†	jet fire	N	4 – 6	2.1 – 3.2
Bryan	12.7 mm oak	none†	jet fire	N	6 – 8	1.6 – 2.1
Sanderson	12.7+15.9 mm plywood	N.A.	bonfire above	N	35.0	0.82
Sanderson	12.7+15.9 mm plywood	N.A.	bonfire below	N	35.0	0.82
Mittendorf	12.7 mm plywood	unknown	liquid/wood	Y	2.0	6.4
Straseske	19 mm waferboard	T&G	liquid	Y	6.83 – 9.0	2.1 – 2.8

* - only on long sides; butt edges on short sides
† - small-scale samples in one solid piece

Appendix D - SAP2000 Description

Overview:

SAP2000 is a stand-alone finite-element-based structural program for the analysis and design of civil structures. It offers an intuitive, yet powerful user interface with many tools to aid in the quick and accurate construction of models, along with the sophisticated analytical techniques needed to do the most complex projects.

Software Validation:

SAP2000 is object based, meaning that the models are created using members that represent the physical reality. A beam with multiple members framing into it is created as a single object, just as it exists in the real world, and the meshing needed to ensure that connectivity exists with the other members is handled internally by the program. Results for analysis and design are reported for the overall object, and not for each sub-element that makes up the object, providing information that is both easier to interpret and more consistent with the physical structure.

Many tests have been performed to verify the accuracy of this software. Specific results can be viewed in the verification documents located within the software package and from the company website.

Assumptions:

This software uses simplified elements for analysis purposes. It represents beams and columns as finite elements, and it represents slabs as plates or shells. Connections can be given a quantitative stiffness for increased accuracy.

Operations:

SAP2000 is a finite element structural analysis software that has linear, nonlinear, and dynamic capabilities.

Reference:

Wiki: https://wiki.csiamerica.com/display/sap2000/Home

Company: http://www.csiamerica.com/products/sap2000

Appendix E - DHS Condensed Model Study

This section summarizes the key aspects of the DHS Green Building Project structural analysis report. The condensed model study was performed to see if a full light, wood-framed structure could be modeled as a condensed structure by exhibiting planar stress behavior. The following figures represent the simple models used for the planar model study.

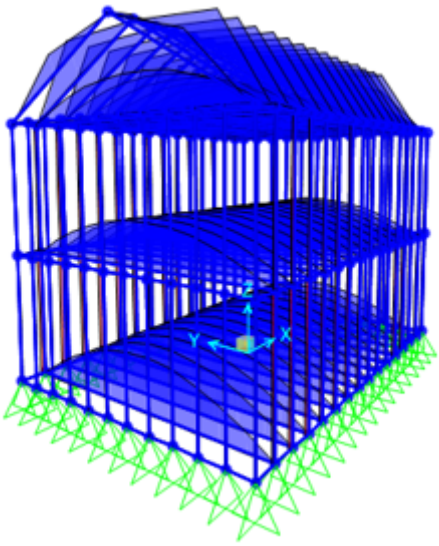

Figure 77 - Full Model

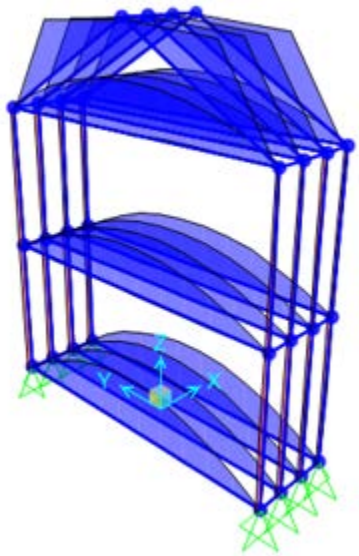

Figure 78 - Condensed Model

The following table represents the summary of moment and stress for the full and condensed models. Both of the models were simplified versions of the house originally chosen as the candidate model for the DHS Green Building Project. The full and condensed models did not contain interior walls for the condensed model study, but it was investigated later into the project. The stress comparison between the full and condensed models yielded similar results to those shown below.

Table 15 - Condensed Study Stress Results

Model Element	Max Moment (k*ft)	Max Stress (ksi)
Element 134 - Full	8640.00	3.840
Element 134 - Condensed	8640.00	3.840

Bibliography

1. Meacham, Brian J. 2014; Available from: http://www.wpi.edu/news/20134/grbldgfire.html.

2. Fahy, Rita, "U.S. Fire Service Fatalities in Structure Fires, 1977-2009", 2010, National Fire Protection Assocation.

3. Peacock, Richard D., Paul A. Reneke, Richard W. Bukowski, and Vytenis Babrauskas. "Defining Flashover for Fire Hazard Calculations." *Fire Safety Journal* 32.4 (1999): 331-45. Web.

4. Stern-Gottfried, Jamie, Guillermo Rein, Luke A. Bisby, and Jose L. Torero. "Experimental Review of the Homogeneous Temperature Assumption in Post-flashover Compartment Fires." *Fire Safety Journal* 45.4 (2010): 249-61. Web.

5. Buchanan, Andrew Hamilton. *Structural Design for Fire Safety*. Chichester: Wiley, 2002. Print.

6. *NDS, National Design Specification for Wood Construction ASD/LRFD*. Washington, D.C.: American Forest & Paper Association, 2005. Print.

7. Illston, J. M., J. M. Dinwoodie, and A. A. Smith. *Concrete, Timber, and Metals: The Nature and Behaviour of Structural Materials*. New York: Van Nostrand Reinhold, 1987. Print.

8. Albano, Leonard D., “CE 534 - Structural Design for Fire Conditions”, class notes, Class 5, February 9, 2006.

9. Lie, T. T. *Structural Fire Protection: Manual of Practice*. New York, NY: American Society of Civil Engineers, 1992. Print.

10. "Online Certifications Directory." *UL*. N.p., n.d. Web. 20 Apr. 2016. <database.ul.com>.

11. *Standard Test Methods for Fire Tests of Building Construction and Materials*. West Conshohocken, PA: ASTM International, 2008. Print.

12. *Fire-resistance Tests: Elements of Building Construction*. Geneva: ISO, 2000. Print.

13. *Calculating the Fire Resistance Exposed Wood Members*. Washington, DC: American Forest & Paper Association, American Wood Council, 2015. Print.

14. Babrauskas, Vytenis. "Charring Rate of Wood as a Tool for Fire Investigations." *Fire Safety Journal* 40.6 (2005): 528-54. Web.

15. Batel, Mehdi. *Operational Modal Analysis – Another Way of Doing Modal Testing* (n.d.): n. pag. Web. <http://www.sandv.com/downloads/0208batl.pdf>.

16. Figueroa, Michael J. *Quantification of Green Building Features on Firefighters: DHS Structural Report.* 2015. Pending.

17. Martin, Drew. *Quantification of Green Building Features on Firefighters: Experimental Plan for Structural Fire Tests at WPI.* 2014 Pending.

18. *Minimum Design Loads for Buildings and Other Structures*. Reston, VA: Published by American Society of Civil Engineers, 2013. Print.

19. HUD, "Residential Structural Design Guide: 2000 Edition ", 2000: U.S. Department of Housing and Urban Development.

20. "SAP2000 | Computers and Structures, Inc." *Computers and Structures, Inc.*N.p., n.d. Web. 14 Apr. 2015.

21. "Thermal Expansion." (n.d.): n. pag. ASM International. Web. 14 Apr. 2015. <http://www.owlnet.rice.edu/~msci301/ThermalExpansion.pdf>.

22. Birk, A. M., and Jonathan D. J. Vandersteen. "The Survivability of Steel and Aluminum 33.5 Pound Propane Cylinders in Fire." *Process Safety Progress Proc. Safety Prog.* 22.2 (2003): 129-35. Web.

23. McGrattan, Kevin, Simo Hostikka, Randall McDermott, Jason Floyd, Craig Weinschenk, and Kristopher Overholt. *Fire Dynamics Simulator User's Manual*. Gaithersburg, MD: U.S. Dept. of Commerce, Technology Administration, National Institute of Standards and Technology, 2000. Print.

24. Chopra, Anil K. *Dynamics of Structures: Theory and Applications to Earthquake Engineering*. Englewood Cliffs, NJ: Prentice Hall, 1995. Print.

25. The Modal Shop, Inc. *The Fundamentals of Modal Testing*. Application Note 243-3. <http://www.modalshop.com/techlibrary/Fundamentals%20of%20Modal%20Testing.pdf>